Elsevier Editorial System(tm) for Journal of Luminescence
Manuscript Draft

Manuscript Number: LUMIN-D-14-00570R2

Title: Further studies on the relationship between IRSL and BLSL at relatively high temperatures for potassium-feldspar from sediments

Article Type: Research Paper

Section/Category: LED/OLED phosphors + phosphors + scintillator/thermoluminescence/dosimetry/afterglow

Keywords: K-feldspar; IRSL; BLSL; component

Corresponding Author: Dr. Sheng-Hua Li,

Corresponding Author's Institution: The University of Hong Kong

First Author: Zhijun Gong

Order of Authors: Zhijun Gong; Bo Li; Sheng-Hua Li

Abstract: In optical dating of potassium-feldspar, the luminescence signals can be stimulated by both infrared (IR) light and blue light (BL). To develop reliable dating methods using different stimulation light sources for feldspars, it is important to understand the sources of the traps associated with the infrared stimulated luminescence (IRSL) and blue light stimulated luminescence (BLSL) and their relationship. In this study, we explored the luminescence characteristics of IRSL and BLSL at different stimulation temperatures (from 60 °C to 200 °C) and their relationship based on five sets of experiments, i.e. post-IR BLSL, post-BL IRSL experiments, pulse annealing test, dose response test and laboratory fading rate test. Our results suggest that the luminescence characteristics of IRSL and BLSL and their relationship are dependent on stimulation temperature. For IR stimulation at a relatively high temperature of 200 °C, at least two components of IRSL signals are involved in the process. One component of IRSL signals can be easily bleached by BL stimulation at 60 °C, while the other is relatively hard to be bleached by BL stimulation at 60 °C. The two components have different luminescence properties, such as thermal stability, dose response and laboratory fading rate.

*Marked Manuscript
Click here to download Marked Manuscript: Marked change on 2nd revision.docx Click here to view linked References

Further studies on the relationship between IRSL and BLSL at relatively high temperatures for potassium-feldspar from sediments

Zhijun Gong[a,b], Bo Li[a,c], Sheng-Hua Li[a,*]

[a] Department of Earth Sciences, The University of Hong Kong, Pokfulam Road, Hong Kong, China

[b] Key laboratory of Cenozoic Geology and Environment, Institute of Geology and Geophysics, Chinese Academy of Sciences, Beijing, China

[c] Centre for Archaeological Science, School of Earth and Environmental Sciences, University of Wollongong, Wollongong, NSW 2522, Australia

*Corresponding author: shli@hku.hk

Abstract:

In optical dating of potassium-feldspar, the luminescence signals can be stimulated by both infrared (IR) light and blue light (BL). To develop reliable dating methods using different stimulation light sources for feldspars, it is important to understand the sources of the traps associated with the infrared stimulated luminescence (IRSL) and blue light stimulated luminescence (BLSL) and their relationship. In this study, we explored the luminescence characteristics of IRSL and BLSL at different stimulation temperatures (from 60 °C to 200 °C) and their relationship based on five sets of experiments, i.e. post-IR BLSL, post-BL IRSL experiments, pulse annealing test, dose response test and laboratory fading rate test. Our results suggest that the luminescence characteristics of IRSL and BLSL and their relationship are dependent on stimulation temperature. For IR stimulation at a relatively high temperature of 200 °C, at least two components of IRSL signals are involved in the process. One component of IRSL signals can be easily bleached by BL stimulation at 60 °C, while the other is relatively hard to be bleached by BL stimulation at 60 °C. The two components have different luminescence properties, such as thermal stability, dose response and laboratory fading rate.

Keywords: K-feldspar, IRSL, BLSL, component

1. Introduction

Both quartz and potassium-rich feldspar (K-feldspar) have been widely used as natural dosimeters for optically stimulated luminescence (OSL) dating (Aitken, 1998). Compared with quartz OSL, the infrared stimulated luminescence (IRSL) signal from K-feldspar (Hütt et al., 1988) has advantages of much brighter luminescence signals and much higher dose saturation level, making feldspar as an attractive candidate for luminescene dating of the natural sedimentary samples. However, the usage of K-feldspar for dating has long been hindered by the anomalous fading of the trapped charges related to the IRSL signals (e.g. Spooner, 1994; Huntley and Lamonthe, 2001; Li and Li, 2008).

More recently, progress in understanding anomalous fading in feldspar has raised the prospect of isolating a non-fading component from the IRSL at relatively high temperatures (Thomsen et al., 2008; Li, 2010; Jain and Ankjærgaard, 2011; Li and Li, 2013). Correspondingly, a two-step post IR IRSL (pIRIR) protocol (Buylaert et al., 2009; Thiel et al., 2011) and a multi-elevated-temperature post-IR IRSL (MET-pIRIR) protocol (Li and Li, 2011a) have been proposed to overcome anomalous fading for dating K-feldspar from sediments, which offer the promising potential for extending the luminescence dating limit (Thiel et al., 2011; Li and Li, 2012; Li et al., 2013, However, the high temperature pIRIR signal~~s~~ (e.g. >200 °C) is~~are~~ found to be more difficult to bleach than the IRSL signal~~s~~ measured at lower temperatures (Li and Li, 2011a; Buylaert et al., 2012; Murray et al., 2012), and it usually requires up to several hours or even days of exposure to sunlight or a solar simulator to bleach the pIRIR signal~~s~~ down to a stable level (here the term "bleach" means to reduce the luminescence intensity by optical stimulation). For some samples, a significant non-bleachable (or residual) component in the pIRIR signals was left even after a prolonged bleaching period using solar simulator or sunlight (Buylaert et al., 2011; Lowick et al., 2012; Chen et al., 2013; Li et al., 2014b). These studies suggest that the IRSL signals recorded at relatively high temperature have different luminescence behavior compared with the IRSL signals at room temperature.

There have been several studies conducted to explore the relationship between

luminescence with IR stimulation and luminescence with visible wavelength light stimulation. It was demonstrated that the majority of green light stimulated luminescence (GLSL) can be bleached by prolonged IR light and an upper limit of ~ 90% GLSL was depleted as a result of IR bleaching at room temperature (Duller and Bøtter-Jensen, 1993; Galloway, 1994). Jain and Singhvi (2001) concluded that the blue-green (BG) stimulated luminescence measured at 125 °C is associated with at least two trap populations. One trap population is responsive to both IR stimulation and BG stimulation. Another trap population is only responsive to BG stimulation. Gong et al. (2012) conducted a study on the relationship between the infrared stimulated luminescence (IRSL) and blue light stimulated luminescence (BLSL) at 60 °C. They observed that most of the IRSL signals at 60 °C can be bleached by BL at 60 °C, while the BLSL signals at 60 °C can only be partially bleached by IR at 60 °C. The sources for the IRSL at 60 °C are mainly associated with the fast and medium components of the BLSL at 60 °C.

In this study, in order to better understand the sources of the traps associated with the IRSL and BLSL, we further explore the relationship between IRSL and BLSL using K-feldspar from two aeolian sand samples. The luminescence properties, in terms of thermal stability, dose response and laboratory fading rate, are also examined for the different IRSL components at a relatively high temperature of 200 °C.

2. Samples and equipment

Two aeolian sand samples (HSDK-11 and SY) from the Hunshandake desert in northeast China were used in this study. Both samples have been investigated in previous studies (Li et al., 2002; Gong et al., 2013). The samples are from the same environmental settings of the same region and have similar luminescence behaviors, so the experimental results obtained from them should be comparable. The samples were treated with 10 % hydrochloric acid (HCl) and 10 % hydrogen peroxide (H_2O_2) to remove carbonate and organic matter, respectively, in subdued red light in the

Luminescence Dating Laboratory, the University of Hong Kong. Grains of 150-180 μm in diameter were obtained by dry sieving. The K-feldspar grains were separated with heavy liquids (2.58 $g \cdot cm^{-3}$) and then etched for 40 min with diluted (10 %) hydrofluoric acid (HF) to clean the grains. HCl (10 %) was used again to dissolve any contaminating fluorides after etching before final rinsing and drying. K-feldspar grains were prepared by mounting the grains in a monolayer, on a 9.8 mm diameter aluminum disc with "Silkospay" silicone oil.

The luminescence measurements of the sample HSDK-11 were carried out with an automated Risø TL-DA-15 reader equipped with an IR LED array (880 nm, FWHM 40 nm) and a blue LED array (470 nm, FWHM 20 nm) in the Luminescence Dating Laboratory, the University of Hong Kong. The IR and BL stimulations deliver ~135 $mW \cdot cm^{-2}$ and ~50 $mW \cdot cm^{-2}$ at the sample position, respectively (Bøtter-Jensen et al., 2003). To keep our results comparable with those from Gong et al. (2012), 90% of the full power was used for stimulation in this study. Irradiations were carried out within the reader using a $^{90}Sr/^{90}Y$ beta source which delivered a dose rate of 0.0761 $Gy \cdot s^{-1}$ to K-feldspar on aluminum discs. The IRSL and the BLSL signals were both detected after passing through 7.5-mm-thick U-340 filters, which mainly pass light from 290 nm to 370 nm with peak transmission at ~340 nm (Li et al., 2007b). The experimental work on the other sample SY was performed in the Luminescence Dating Laboratory, Institute of Geology and Geophysics, Chinese Academy of Sciences. The luminescence measurements of the sample SY were carried out with an automated Risø TL/OSL reader (TL/OSL-DA-15) using the similar equipment setting. The $^{90}Sr/^{90}Y$ beta source in the equipment delivered a dose rate of 0.0837 $Gy \cdot s^{-1}$ to K-feldspar on aluminum discs.

3. Experimental details and results

3.1 The relationship between the IRSL and the BLSL at different stimulation temperatures

Two sets of experiments, namely post-IR BLSL (pIR-BLSL) and post-blue light IRSL (pBL-IRSL), are conducted to investigate the relationship between the IRSL and the BLSL at different stimulation temperatures. For simplification, we describe the stimulation temperatures used in the prior IR and post-IR BLSL as pIR(T_1)-BLSL(T_2), where T_1 is the stimulation temperature used in the prior IR measurement and T_2 is the temperature used in post-IR BLSL measurement.

3.1.1 pIR-BLSL experiments

The pIR-BLSL experiments were carried out using the procedure listed in Table 1. Four aliquots of of K-feldspar grains HSDK-11 were firstly heated to 500 °C and then given a dose of 30.4 Gy. These aliquots were subsequently preheat at 280 °C for 10 s and then bleached using IR stimulation at a temperature of T_1 for different periods ranging from 0 to 5000 s. The pIR-BLSL signal (L_x) was then measured at a temperature of T_2. After that, a test dose of 15.2 Gy was applied and the induced BLSL signal (T_x) was measured following the same preheat to monitor sensitivity change for L_x. The signals for both L_x and T_x were calculated from the integrated photon counts in the first 1 s of stimulation, with subtraction of the instrumental background signal. The experiments are conducted at a set of different temperature combinations, i.e. pIR(60)-BLSL(60), pIR(100)-BLSL(60), pIR(150)-BLSL(60), pIR(200)-BLSL(60) and pIR(200)-BLSL(200), respectively.

The IR bleaching effects on the pIR-BLSL signal for different periods of time are shown in Fig. 1. It is observed that the IR bleaching at higher temperatures can deplete the BLSL at 60 °C at a faster rate than IR stimulation at lower temperatures. The BLSL at 60 °C was bleached to about 5 % of the initial intensity after IR bleaching at 200 °C for 5000 s. In comparison, the BLSL at 60 °C was bleached to about 15 % of the initial intensity after IR bleaching at 60 °C for 5000 s. If we increase the stimulation temperature in BLSL from 60 to 200 °C, i.e. pIR(200)-BLSL (200), the IR stimulation at 200 °C can bleach the most of the traps associated with the BLSL at 200 °C and only 6 % of the initial intensity of the BLSL at 200 °C was

151 remaining after IR bleaching at 200 °C for 5000 s (Fig. 1). The results suggest that
152 both the BLSL measured at 60 °C and the BLSL at 200 °C can only be partially
153 bleached by prolonged (up to 5000 s) IR stimulation even at a relatively high
154 temperature (i.e. 200 °C).

155 In our previous study (Gong et al., 2012), it was found that the BLSL signals
156 measured at 60 °C for the K-feldspar from sample HSDK-11 can be described using
157 three first-order exponential components, which are termed as fast (F), medium (M)
158 and slow (S) components. Gong et al. (2012) demonstrated that the sources for the
159 IRSL at 60 °C are mainly associated with the fast and medium components of the
160 BLSL at 60 °C. To further demonstrate the relationship between IRSL signal at
161 relatively high temperatures and BLSL at 60 °C, the residual BLSL at 60 °C after IR
162 bleaching for different time from 0 s to 5000 s were then fitted using three OSL
163 components. It is found that the pIR-BLSL signals can be well described by the three
164 exponential functions (all $R^2 > 0.96$). The relative ratios of the decay rates of the
165 components of BLSL at 60 °C, i.e. b_f/b_m and b_m/b_s, are calculated at 4.87±0.14 and
166 10.69±0.41, respectively (here the parameters of b_f, b_m and b_s refer to the decay rate
167 of the fast, medium and slow components of BLSL at 60 °C, respectively). It is noted
168 that the assumption of that the BLSL process is first-order may not be true. However,
169 this will not influence our conclusion because it is the relationship between the
170 different parts of BLSL (represented by the fast, medium and slow components) and
171 IRSL that is crucial for our study, rather than whether these components are first-order
172 or not. We, however, acknowledge that there may be some uncertainty associated with
173 the fitting and some results demonstrated by Fig. 2 and Fig. 6 might be partially
174 influenced if these components are not first-order.

175 Fig. 2a illustrates four representative pIR-BLSL signals, which are fitted into three
176 components. The results of IR bleaching for the fast, medium and slow component of
177 BLSL at 60 °C are shown in Fig. 2b. It is observed that the IR stimulation at 200 °C
178 for 5000 s can deplete 99 % of the fast component, ~99 % of the medium component
179 but only ~38 % of the slow component for the BLSL at 60 °C, while IR stimulation at
180 60 °C for 5000 s can only deplete ~97 % of fast component, ~91 % of medium

component and ~12 % of slow component, respectively, for the BLSL at 60 °C. These results indicate that IRSL obtained at 200 °C involves more traps associated with hard-to-bleach components (i.e. the medium and slow components) of BLSL at 60 °C than does the IR stimulation at 60 °C. The results are consistent with previous studies that the IRSL signals at high temperatures (e.g. >200 °C) are relatively harder to bleach than the IRSL at 60 °C (Buylaert et al., 2011; Li and Li, 2011a; Chen et al., 2013).

The relationship between the IRSL and BLSL at different temperatures is further studied by investigating the relationship between the emitted light counts from the IRSL and the corresponding lost counts obtained from the pIR(T_1)-BLSL(T_2) experiments (T_1= 60, 100, 150, 200 °C; T_2= 60, 200 °C). This is similar to the method applied to study the relation between IRSL and thermoluminescence (TL) by Duller (1995). In Fig. 3, we plot the emitted counts from the IRSL, against the corresponding lost counts of the pIR-BLSL as a result of IR bleaching. It is observed that, if the stimulation temperature for IR and BL was identical in both cases (i.e. pIR(60)-BLSL(60) and pIR(200)-BLSL(200)), the emitted counts of the IRSL have a nearly 1:1 relationship with the corresponding lost counts in the pIR-BLSL. However, in the case of T_1>T_2, the emitted counts of the IRSL are larger than the corresponding lost counts in pIR-BLSL, indicating that the relationship between BLSL and IRSL is dependent on the stimulation temperature. It is to be noted that such a relationship between IRSL and BLSL is not influenced by the interference of isothermal TL, because the preheat at 280 °C for 10 s is sufficient to remove any isothermal TL at 200 °C. One straightforward explanation for the temperature dependency of the relationship is that at least two components are involved in the IRSL at the relatively high temperature (such as the IRSL at 200 °C). One component is responsive to the BL at 60 °C. The other is hard to reach by BL at 60 °C, but can be accessed at higher temperatures. The results further support fact that the IRSL signals at relatively high temperatures are relatively harder to bleach than the IRSL at 60 °C (e.g. Chen et al., 2013).

3.1.2 pBL-IRSL experiments

The effects of BL bleaching at 60 °C and 200 °C on the IRSL signals at different temperatures (60, 100, 150 and 200 °C) are investigated using pBL-IRSL experiments (see the procedures listed in Table 1). The experiments conducted are pBL(60)-IRSL(60), pBL(60)-IRSL(100), pBL(60)-IRSL(150), pBL(60)-IRSL(200) and pBL(200)-IRSL(200), respectively. Four aliquots of K-feldspar grains of HSDK-11 were firstly heated to 500 °C to remove any residual signals and then given the same irradiation dose of 30.4 Gy. These aliquots were then held at 280 °C for 10 s. They were subsequently bleached with BL at 60, 200 °C for different periods from 0 to 320 s before IRSL measurements. After that, the IRSL sensitivity was monitored and measured following a test dose of 15.2 Gy and preheat at 280 °C for 10 s.

The remnant IRSL at different temperatures (50, 100, 150 200 °C) as a result of BL bleaching at 60, 200 °C for different periods of times are shown in Fig. 4. It is demonstrated that the IRSL at 60 °C can be bleached to a negligible level (~0.2 %) by BL stimulation at 60 °C for 320 s, while 3.5 % of the initial IRSL at 200 °C still remains after BL bleaching at 60 °C for 320 s. These results indicate that, compared with the IRSL at 60 °C, the IRSL at 200 °C involves more traps that are harder to bleach by BL at 60 °C. However, the IRSL at 200 °C can be bleached to a negligible level (~0.2 %) by BL stimulation at 200 °C for 320 s. In addition, the decay rates in the pBL(200)-IRSL (200) and the pBL(60)-IRSL(60) are very similar and they are calculated at 0.23 ±0.02 s^{-1} and 0.21 ±0.01 s^{-1}, respectively. These results further suggest that the relationship between the IRSL and the BLSL is dependent on stimulation temperature.

Further investigation is made on the relationship between the emitted counts from the BLSL and the corresponding lost counts from pBL(T_1)-IRSL(T_2) (T_1= 60, 200 °C; T_2= 60, 100, 150, 200 °C) (Fig. 5). It is observed that the emitted counts from the BLSL measured both at 60 °C and at 200 °C are significantly larger than the corresponding lost counts from pBL(T_1)-IRSL(T_2). These results indicate that BL can

access much more traps than IR stimulation. Only part of traps associated with the BLSL at 60 °C and at 200 °C is accessible by IR stimulation, which is similar to the results of IRSL observed at 60 °C (Gong et al, 2012). It is also demonstrated that relationship between emitted BLSL counts and lost counts of pBL-IRSL changes as the stimulation temperature changes.

To further demonstrate the relationship between different OSL components of the BLSL signal at 60 °C and the IRSL signals at relatively high temperatures, the emitted light counts from different OSL components of the BLSL signal at 60 °C are compared with the corresponding lost counts from the pBL(60)-IRSL(200) and pBL(60)-IRSL(60) as a result of BL bleaching at 60 °C for different periods. We plot the emitted counts from the various OSL components of the BLSL at 60 °C, against the lost counts of IRSL at 60 °C and IRSL at 200 °C as a result of BL bleaching in Fig. 6. It is observed that the lost counts in pBL(60)-IRSL(200) are larger than the sum of the emitted light counts of the fast and medium components of BLSL at 60 °C, while the lost counts in pBL(60)-IRSL(60) have a nearly 1:1 relationship with the sum of the emitted light counts of the fast and medium components of BLSL at 60 °C. These results indicate that the IRSL signals at 200 °C are involved with not only the fast and medium components of BLSL at 60 °C, but also some other OSL components (e.g. slower components of BLSL at 60 °C). In contrast, there is a close relationship between IRSL at 60 °C and the fast and medium components of BLSL at 60 °C (Gong et al., 2012). The results are consistent with the observations in previous section 3.1.1.

In summary, the results from the pIR-BLSL and pBL-IRSL bleaching experiments suggest that the relationship between IRSL and BLSL is dependent on stimulation temperature. At least two components of traps are involved in the IRSL measured at elevated temperatures (e.g., 200 °C). One component can be easily bleached by BL at 60 °C, and the other of the IRSL is relatively harder to access by BL at 60 °C. The results show that the IRSL signals at relatively high temperatures are harder to be bleached than the IRSL at room temperature.

3.2 Luminescence properties of IRSL at relatively high temperature

The luminescence characteristics of the IRSL at 200 °C, the pIR(60)-IRSL(200) and the pBL(60)-IRSL(200), including thermal stability, dose response and laboratory fading rate, were further investigated. In both the pIR(60)-IRSL(200) and the pBL(60)-IRSL(200) experiments, the IR and BL bleaching time was both fixed at 200 s.

3.2.1 Thermal stability study

The thermal stability studies are carried out using the pulse annealing test (Table 2) (Li et al., 1997; Li and Tso, 1997). The tests were conducted for the IRSL at 60 °C, the IRSL at 200 °C, the pIR(60)-IRSL(200) and the pBL(60)-IRSL(200), respectively. An aliquot of K-feldspar of SY was firstly heated to 500 °C and then given an irradiation dose of 30.4 Gy. After that, it was preheated at 280 °C for 10 s and then heated to a temperature at T °C before the remaining IRSL was measured at 60 °C for 160 s. The sensitivity change was monitored by measuring the IRSL signal at 60 °C from a test dose of 30.4 Gy. The same preheat condition (280 °C for 10 s) was applied for the test dose IRSL measurement. This cycle was repeated by increasing the annealing temperature (T) from 160 °C to 500 °C in steps of 20 °C. The similar pulse annealing test procedures were also conducted for the IRSL at 200 °C, the pIR(60)-IRSL(200) and the pBL(60)-IRSL(200) (Table 2). The heating rate for all these pulse annealing experiments was 3 $°C \cdot s^{-1}$.

The typical decay curve of the pBL(60)-IRSL(200) signal is shown in Fig. 7. The results of the pulse annealing test of the IRSL at 60 °C, the IRSL at 200 °C, the pIR(60)-IRSL(200) and the pBL(60)-IRSL(200) are shown in Fig. 8. It is observed that the thermal stability of the IRSL at 200 °C is relatively more stable than that of the IRSL at 60 °C. Li and Li (2011b; 2013) also observed the different thermal stabilities among the IRSL at different stimulation temperatures. In addition, it is found that both pIR(60)-IRSL(200) and pBL(60)-IRSL(200) is more thermally stable than IRSL at 200 °C. The results suggest that at least two components are involved in

300 the IRSL at 200 °C and the components have significantly different thermal stability.
301 Both IR at 60 °C and BL at 60 °C can remove the thermally relatively unstable
302 component of IRSL 200 °C. It is interesting to be noted that the pBL(60)-IRSL(200)
303 is significantly more thermally stable than pIR(60)-IRSL(200), indicating that the BL
304 at 60 °C is more efficient than IR at 60 °C to reduce thermally unstable component in
305 the IRSL at 200 °C.
306
307 3.2.2 Dose response curves
308
309 Different shapes of dose response curve (DRC) may provide an indication of
310 different origins of different luminescence signals (Gong et al., 2012). Here we
311 compare the DRC of the IRSL at 200 °C from K-feldspar with that of the
312 pBL(60)-IRSL(200). Regenerative doses ranging from 0 to 1950 Gy were employed
313 in a single aliquot regeneration (SAR) protocol for the IRSL at 200 °C. A test dose of
314 52 Gy was applied and the test dose signal (T_x) was measured to monitor and correct
315 for sensitivity change. A recycle dose at 26 Gy was used and the recycling ratios all
316 fall within the range of 1.0 ± 0.05 for the sample. The preheat temperature (held at
317 280 °C for 10 s) was the same for regeneration and test dose measurements. A
318 cut-heat to 500 °C was used between each of the SAR cycles to clean the residual
319 signals from the previous cycle. The IRSL signals L_x and T_x were calculated from the
320 integrated photon counts in the first 1 s of stimulation, with subtraction of a
321 background signal derived from the last 10 s of the 160 s stimulation. For construction
322 the DRC of the pBL(60)-IRSL(200), a similar SAR procedure was applied, except
323 that a BL bleaching at 60 °C for 200 s was added before each IRSL measurement for
324 both the regenerative and test dose measurements. The dose response curves for the
325 two signals are shown in Fig. 9. It is found that the pBL(60)-IRSL(200) signal have a
326 different dose saturation level with the IRSL at 200 °C.
327 If the two dose response curves are fitted with double saturation exponential
328 function (equation 1),

$$I = I_0 + I_a(1-\exp(-D/D_{0,a})) + I_b(1-\exp(-D/D_{0,b})) \quad (1)$$

The dose saturation level of two D_0 ($D_{0,a}$ and $D_{0,b}$) parameters are 42.9±5.8 Gy and 289.7±22.4 Gy for the pBL(60)-IRSL(200) signal, while the values of two D_0 ($D_{0,a}$ and $D_{0,b}$) parameters of the IRSL at 200 °C are significantly higher at 214.6±9.9 Gy and 806.1±69.6 Gy, respectively. The results indicate that at least two components are involved in the IRSL at elevated temperature. One group is easy to bleach by BL at 60 °C and they have a higher dose saturation level, while the other group is hard to bleach by BL at 60 °C and they have a lower dose saturation level.

3.2.3 Laboratory fading test

Anomalous fading was observed for both IRSL and BLSL signals in previous studies (e.g. Thomsen et al., 2008). Here we studied the laboratory fading rates for the IRSL at 200 °C, the pIR(60)-IRSL(200) and the pBL(60)-IRSL(200) signals. In measurement of the IRSL at 200 °C, six aliquots of SY were heated to 500 °C to remove any residual signals (similar to a hot-bleach between SAR cycles). Then these aliquots were given 50.8 Gy and immediately preheated at 280 °C for 10 s. The sensitivity corrected signals were then measured after delays of different periods. For the test dose, 12.7 Gy was given and the same preheat condition was applied. The IRSL signals $L_{(x)}$ and $T_{(x)}$ were calculated from the integrated photon counts in the first 1 s of stimulation, with subtraction of a background signal derived from the last 10 s of the 160 s stimulation. The first measurement of the IRSL at 200 °C signal took place at a time t_c= 562 s after the mid-point of the irradiation time. A similar measurement procedure was adopted for measuring the fading rate for the pIR(60)-IRSL(200) and pBL(60)-IRSL(200) signals. For the pIR(60)-IRSL(200) signal, an IR bleaching at 60 °C for 200 s was added before the IRSL measurement at 200 °C for both the regenerative and test dose measurements. The first measurement of the pIR(60)-IRSL(200) signal took place at a time t_c= 669 s after the mid-point of

357 the irradiation time. For the pBL(60)-IRSL(200) signal, a BL bleaching at 60 °C for
358 200 s was added before the IRSL measurement at 200 °C for both the regenerative
359 and test dose measurements. The first measurement of the pBL(60)-IRSL(200) signal
360 took place at a time t_c= 669 s after the mid-point of the irradiation time. The decay of
361 the IRSL at 200 °C, the pIR(60)-IRSL(200) and the pBL(60)-IRSL(200) signals after
362 normalization as a function of storage time is shown in Fig 10. The corresponding
363 anomalous fading rates (g-value) are calculated based on the data sets and are also
364 shown in Fig. 10. It is observed that the IRSL at 200 °C, the pIR(60)-IRSL(200) and
365 the pBL(60)-IRSL(200) have significantly different laboratory fading rates. The g
366 value for the IRSL at 200 °C was detected at 4.0±0.3 %/decade, the g value of the
367 pIR(60)-IRSL(200) was at 1.6±0.4 %/decade and the pBL(60)-IRSL(200) was 0.4±
368 0.4 %/decade. This result indicates that there are at least two components for the IRSL
369 at 200 °C. One component is easy to bleach by IR at 60 °C and BL at 60 °C and it has
370 higher laboratory fading rate, while the other is hard to bleach by IR at 60 °C and BL
371 at 60 °C and it has a significantly lower fading rate.
372
373 ## 4. Discussion
374 The sources and process of the traps associated with IRSL from feldspar are
375 important for developing reliable dating methods. Different models have been
376 proposed to explain the various luminescence behaviors of feldspars. A single trap
377 model has been proposed recently to explain the luminescence characteristics for
378 feldspar (e.g., Jain and Ankjærgaard, 2011; Anderson et al., 2012), while a multi-trap
379 model is suggested alternatively by others (e.g., Duller and Bøtter-Jensen, 1993; Li
380 and Li, 2011; Thomsen et al., 2011; Li et al., 2014). These studies were based on their
381 own experimental designs with limited experimental conditions and the explanations
382 are based on different assumptions, so a unique interpretation cannot be reached. It is
383 hoped that the study of the relationship between BLSL and IRSL could be helpful for
384 understanding the source and process of IRSL, because, unlike IRSL process, BLSL is
385 expected to be a simpler and delocalized process due to the higher photon energy of

BL (~2.64 eV) compared to the main IRSL trap depth (~2.5 eV) (e.g. Baril and Huntley, 2003; Kars et al., 2013). Based on our results, we are in favor of the multiple-trap model to explain the experimental data obtained in this study, which cannot be well explained using a simple single-trap model. The pieces of evidence~~s~~ are given as follows:

(1) If we assume that IRSL at 200 °C and 60 °C originate the same traps and then both signals should be depleted by BL at a similar rate, because BL have energy high enough to evict the trapped electron to the conduction band and then the electron can randomly recombine with both close and distant holes. In Fig. 4, it is clearly shown~~ed~~ that, compared with the IRSL at 60 °C, the IRSL at 200 °C is bleached at the significantly slower rate by BL at 60 °C, suggesting that IRSL signals at 200 °C are involved with traps which are very hard to bleach by BL at 60 °C. This could be due to either that the hard-to-bleach component has a deeper trap depth (>2.5 eV) or that the component has a different photoionization cross-section, which both indicate a different trap from the easy to bleach component.

(2) During the pIR(60)-BLSL(60) experiments, the emitted counts of the IRSL have a nearly 1:1 relationship with the corresponding lost counts in the pIR-BLSL. However, this is not the case for the pIR(200)-BLSL(60) (Fig. 3). This indicates that IRSL at elevated temperature can access more traps that are more difficult to bleach by BL at 60 °C.

(3) The pBL(60)-IRSL(200) and IRSL signals at 200 °C have very different luminescence properties, such as thermal stability, dose response and fading rate. Since BL have energy high enough to evict the trapped electron to the conduction band, the electron will randomly recombine with close or distant holes after excitation. Hence, BL will cause not only recombination of spatially close electron-hole pairs, but also recombination of distant electron-hole pairs. As a result, BL bleaching should not change the relative proportions between close and distant electron-hole pairs. Correspondingly, it is expected that the pBL-IRSL should have a similar thermal stability as IRSL, and the pIR-IRSL should have a higher thermal stability than pBL-IRSL. Our results, however, showed that the pBL(60)-IRSL(200) is significantly

more thermally stable than both the IRSL at 200 °C and pIR(60)-IRSL(200) (Fig. 8), which cannot be explained by the single-trap model. Similarly, a similar fading rate should be expected for the IRSL(200) and pBL(60)-IRSL(200) signals based on a single-trap model. For our samples, the g values for the IRSL at 200 °C are greatly reduced after the BL bleaching at 60 °C for 200 s (Fig. 10). It is interesting to be noted that the laboratory fading rate of pBL(60)-IRSL(200) is significantly lower than that of pIR(60)-IRSL(200), suggesting that the BL at 60 °C is more efficiently than the IR at 60 °C to remove spatially close electron-hole pairs (easy-to-fade), which cannot be explained by a single trap model.

Based on the above arguments, we think that a single trap model is not sufficient to explain all the luminescence phenomena in feldspar. In the future, it is maybe helpful to use time-resolved optically stimulated luminescence (TR-OSL) technique to further study the luminescence behaviors of K-feldspar (e.g. Chithambo and Galloway, 2001).

Another outcome of our study is that we first demonstrate that the pBL(60)-IRSL(200) has a high thermal stability and a negligible fading rate, which opens the potential of using this signal in sediments dating without the corrections for anomalous fading. A potential advantage of using pBL(60)-IRSL(200) is that blue bleaching at 60 °C can eliminate the contribution of quartz grains to IRSL at elevated~~ion~~ temperatures (Fan et al., 2009). Quartz grains can coexist with K-feldspar after heavy liquid separation. The IRSL of quartz at elevated~~ion~~ temperatures can be effectively bleached by blue light at low temperatures, but not by infrared. Further tests on the applicability in dating are required to confirm the suitability of using the pBL-IRSL at relatively high temperatures.

5. Conclusions

From the pIR-BLSL and pBL-IRSL bleaching experiments, it is concluded that the relationship between IRSL and BLSL is dependent on the stimulation temperature. If stimulation temperatures for the IRSL increase from 60 to 200 °C, at least two

components are associated with the IRSL at 200 °C. One component is easy to bleach by BL at 60 °C, and the other relative hard to bleach by BL at 60 °C. The two components of the IRSL at 200 °C have significantly different luminescence properties, in terms of thermal stability, dose saturation level and laboratory fading rates.

Acknowledgments

This study was financially supported by the grants to Sheng-Hua Li from the Research Grant Council of the Hong Kong Special Administrative Region, China (Project nos. 7028/08P and 7033/12P). The authors are grateful to the two anonymous reviewers for providing valuable comments and suggestions on the manuscript.

476

477 Reference

478 Adamiec, G., 2005. OSL decay curves—relationship between single- and
479 multiple-grain aliquots. Radiation Measurements 39, 63-75.

480 Aitken, M.J., 1998. An Introduction to Optical Dating. Oxford Unversity Press,
481 Oxford.

482 Andersen, M.T., Jain, M., Tidemand-Lichtenberg, P., 2012. Red-IR stimulated
483 luminescence in K-feldspar: Single or multiple trap origin? Journal of Applied
484 Physics 112, 043507, DOI 10.1063/1.4745018.

485 Bøtter-Jensen, L., Andersen, C.E., Duller, G.A.T., Murray, A.S., 2003. Developments
486 in radiation, stimulation and observation facilities in luminescence measurements.
487 Radiation Measurements 37, 535-541.

488 Baril, M. R., and Huntley, D. J., 2003, Optical excitation spectra of trapped electrons
489 in irradiated feldspars: Journal of Physics-Condensed Matter, v. 15, no. 46, p.
490 8011-8027.

491 Buylaert, J.P., Jain, M., Murray, A.S., Thomsen, K.J., Thiel, C., and Sohbati, R., 2012,
492 A robust feldspar luminescence dating method for Middle and Late Pleistocene
493 sediments. Boreas 41, 435-451.

494 Buylaert, J.P., Murray, A.S., Thomsen, K.J., Jain, M., 2009. Testing the potential of an
495 elevated temperature IRSL signal from K-feldspar. Radiation Measurements 44,
496 560-565.

497 Buylaert, J.P., Thiel, C., Murray, A., Vandenberghe, D.G., Yi, S., Lu, H., 2011. IRSL
498 and post-IR IRSL residual doses recorded in modern dust samples from the
499 Chinese Loess Plateau. Geochronometria 38, 432-440.

500 Chen, Y., Li, S.-H., Li, B., 2013. Residual doses and sensitivity change of post IR
501 IRSL signals from potassium feldspar under different bleaching conditions.
502 Geochronometria 40, 229-238.

503 Chithambo, M.L., Galloway, R.B., 2001. On the slow component of luminescence
504 stimulated from quartz by pulsed blue light-emitting diodes. Nuclear Instruments
505 and Methods in Physics Research Section B: Beam Interactions with Materials

and Atoms 183, 358-368.

Duller, G.A.T., 1995. Infrared bleaching of the thermoluminescence of four feldspars. Journal of Physics D: Applied Physics 28, 1244.

Duller, G.A.T., Bøtter-Jensen, L., 1993. Luminescence from Potassium Feldspars Stimulated by Infrared and Green Light. Radiation Protection Dosimetry 47, 683-688.

Fan, A.C., Li, S.-H., Li, B., 2009. Characteristics of quartz infrared stimulated luminescence (IRSL) at elevated temperatures. Radiation Measurements 44, 434-438.

Galloway, R.B., 1994. Comparison of the green- and infrared-stimulated luminescence of feldspar. Radiation Measurements 23, 617-620.

Gong, Z., Li, B., Li, S.-H., 2012. Study of the relationship between infrared stimulated luminescence and blue light stimulated luminescence for potassium-feldspar from sediments. Radiation Measurements 47, 841-845.

Gong, Z., Li, S.-H., Sun, J., Xue, L., 2013. Environmental changes in Hunshandake (Otindag) sandy land revealed by optical dating and multi-proxy study of dune sands. Journal of Asian Earth Sciences 76, 30-36.

Hütt, G., Jaek, I., Tchonka, J., 1988. Optical Dating: K-Feldspars Optical Response Stimulation Spectra. Quaternary Science Reviews 7, 381-385.

Huntley, D.J., Lamothe, M., 2001. Ubiquity of anomalous fading in K-feldspars and the measurement and correction for it in optical dating. Canadian Journal of Earth Sciences 38, 1093-1106.

Jain, M., Ankjærgaard, C., 2011. Towards a non-fading signal in feldspar: Insight into charge transport and tunnelling from time-resolved optically stimulated luminescence. Radiation Measurements 46, 292-309.

Jain, M., Singhvi, A.K., 2001. Limits to depletion of blue-green light stimulated luminescence in feldspars: implications for quartz dating. Radiation Measurements 33, 883-892.

Kars, R.H., et al., 2013. On the trap depth of the IR-sensitive trap in Na- and K-feldspar. Radiation Measurements 59, 103-113.

536 Li, B., 2010. The relationship between thermal activation energy, infrared stimulated
537 luminescence and anomalous fading of K-feldspars. Radiation Measurements 45,
538 757-763.
539 Li, B., Jacobs, Z., Roberts, R.G., Li, S.-H., 2013. Extending the age limit of
540 luminescence dating using the dose-dependent sensitivity of MET-pIRIR signals
541 from K-feldspar. Quaternary Geochronology 17, 55-67.
542 Li, B., Jacobs, Z., Roberts, R., Li, S.-H., 2014b, Review and assessment of the
543 potential of post-IR IRSL dating methods to circumvent the problem of anomalous
544 fading in feldspar luminescence. Geochronometria, 41, 178-201.
545 Li, B., Li, S.-H., 2008. Investigations of the dose-dependent anomalous fading rate of
546 feldspar from sediments. Journal of Physics D-Applied Physics 41, 225502.
547 Li, B., Li, S.-H., 2011a. Luminescence dating of K-feldspar from sediments: A
548 protocol without anomalous fading correction. Quaternary Geochronology 6,
549 468-479.
550 Li, B., Li, S.-H., 2011b. Thermal stability of infrared stimulated luminescence of
551 sedimentary K- feldspar. Radiation Measurements 46, 29-36.
552 Li, B., Li, S.-H., 2012. Luminescence dating of Chinese loess beyond 130 ka using
553 the non-fading signal from K-feldspar. Quaternary Geochronology 10, 24-31.
554 Li, B., Li, S.-H., 2013. The effect of band-tail states on the thermal stability of the
555 infrared stimulated luminescence from K-feldspar. Journal of Luminescence 136,
556 5-10.
557 Li, B., Li, S.-H., Wintle, A.G., Zhao, H., 2007a. Isochron measurements of naturally
558 irradiated K- feldspar grains. Radiation Measurements 42, 1315-1327.
559 Li, B., Roberts, R.G., Jacobs, Z., Li, S.-H., 2014a. A single-aliquot luminescence
560 dating procedure for K-feldspar based on the dose-dependent MET-pIRIR signal
561 sensitivity. Quaternary Geochronology 20, 51-64.
562 Li, S.-H., Chen, Y.Y., Li, B., Sun, J.M., Yang, L.R., 2007b. OSL dating of sediments
563 from desert in northern China. Quaternary Geochronology 2, 23-28.
564 Li, S.-H., Sun, J.M., Zhao, H., 2002. Optical dating of dune sands in the northeastern
565 deserts of China. Palaeogeography Palaeoclimatology Palaeoecology 181,

419-429.

Li, S.-H., Tso, M.Y.W., 1997. Lifetime determination of OSL signals from potassium feldspar. Radiation Measurements 27, 119-121.

Li, S.-H., Tso, M.Y.W., Wong, N.W.L., 1997. Parameters of OSL traps determined with various linear heating rates. Radiation Measurements 27, 43-47.

Lowick, S.E., Trauerstein, M., and Preusser, F., 2012, Testing the application of post IR-IRSL dating to fine grain waterlain sediments. Quaternary Geochronology 8, 33-40.

Murray, A.S., Thomsen, K.J., Masuda, N., Buylaert, J.P., and Jain, M., 2012, Identifying well-bleached quartz using the different bleaching rates of quartz and feldspar luminescence signals: Radiation Measurements 47, 688-695.

Spooner, N.A., 1994. The anomalous fading of infrared-stimulated luminescence from feldspars. Radiation Measurements 23, 625-632.

Thiel, C., Buylaert, J.-P., Murray, A., Terhorst, B., Hofer, I., Tsukamoto, S., Frechen, M., 2011. Luminescence dating of the Stratzing loess profile (Austria) - Testing the potential of an elevated temperature post-IR IRSL protocol. Quaternary International 234, 23-31.

Thomsen, K.J., Murray, A.S., Jain, M., 2011. Stability of IRSL signals from sedimentary K-feldspar samples. Geochronometria 38, 1-13.

Thomsen, K.J., Murray, A.S., Jain, M., Bøtter-Jensen, L., 2008. Laboratory fading rates of various luminescence signals from feldspar-rich sediment extracts. Radiation Measurements 43, 1474-1486.

Figure captions

Figure 1: Remnant BLSL measured at 60 °C and 200 °C after IR bleaching at different temperature for different times. The temperatures for IR bleaching were set at 60, 100, 150 and 200 °C, respectively.

Figure 2: (a) four representative pIR-BLSL signals, which are then deconvoluted into three components. For each of the fitting, the F-statistics are provided and they are all significantly larger than $F_{0.01}$ (e.g. Adamiec, 2005). The corresponding residuals are shown at the right. (b) The residual fast, medium and slow components of BLSL at 60 °C after IR bleaching for different time from 0 s to 5000 s. To better demonstrate the data, the residual fast and medium components of BLSL at 60 °C after IR bleaching for different time from 0 s to 320 s were further shown in the insets, while the y-axis in the insets is on the logarithmic scale. The data were from sample HSDK-11 and the fast, medium and slow components of BLSL at 60 °C were fitted with the decay rates of 0.375±0.004 s^{-1}, 0.077±0.002 s^{-1} and 0.0072±0.0002 s^{-1}, respectively, the same as Gong et al. (2012).

Figure 3: The relationship between emitted counts of the IRSL and the corresponding lost counts of pIR(T_1)-BLSL(T_2) as a result of IR bleaching for different time. T_1= 60, 100, 150, 200 °C, T_2= 60, 200 °C respectively.

Figure 4: Remnant IRSL after blue light bleaching at 60 °C and 200 °C for different times. The temperatures for IR stimulations were set at 60, 100, 150 and 200 °C, respectively.

Figure 5: The relationship between emitted counts of the BLSL and the corresponding lost counts of pBL(T_1)-IRSL(T_2) as a result of blue light bleaching for different time. T_1= 60, 200 °C, T_2= 60, 100, 150, 200 °C, respectively.

622

623 Figure 6: The relationship between emitted counts of OSL components of BLSL at
624 60 °C and the lost counts of pBL(60)-IRSL(200) and pBL(60)-IRSL(60) as a result of
625 blue light bleaching at 60 °C for different times. F+M: The sum of fast and medium
626 components of the BLSL at 60 °C; S: slow component of the BLSL at 60 °C. The data
627 were from sample HSDK-11.

628

629 Figure 7: The typical decay curves of the pBL(60)-IRSL(200) from sample HSDK-11.
630 All the signals were normalized using the initial intensity of the pBL(60)-IRSL(200).

631

632 Figure 8: Pulse annealing curves based on the IRSL signal at 60 °C, the IRSL signal at
633 200 °C, pIR(60)-IRSL(200) and the pBL(60)-IRSL(200) signal; In the
634 pIR(60)-IRSL(200) and pBL(60)-IRSL(200) experiments, the previous IR stimulation
635 and BL stimulation at 60 °C are both at 200 s. The heating rate was 3 $°C \cdot s^{-1}$.

636

637 Figure 9: Dose response curves of the IRSL signal at 200 °C and the
638 pBL(60)-IRSL(200) signal. The two dose response curves could be fitted well by the
639 double saturation exponential function (R^2>0.99; residuals are shown in the inset).

640

641 Figure 10: Anomalous fading tests for IRSL signal at 200 °C, the pIR(60)-IRSL(200)
642 and the pBL(60)-IRSL(200) signal using six aliquots from sample SY as a function of
643 delayed period (t).

644

645

646

647

648

649

650

651

Figure 1

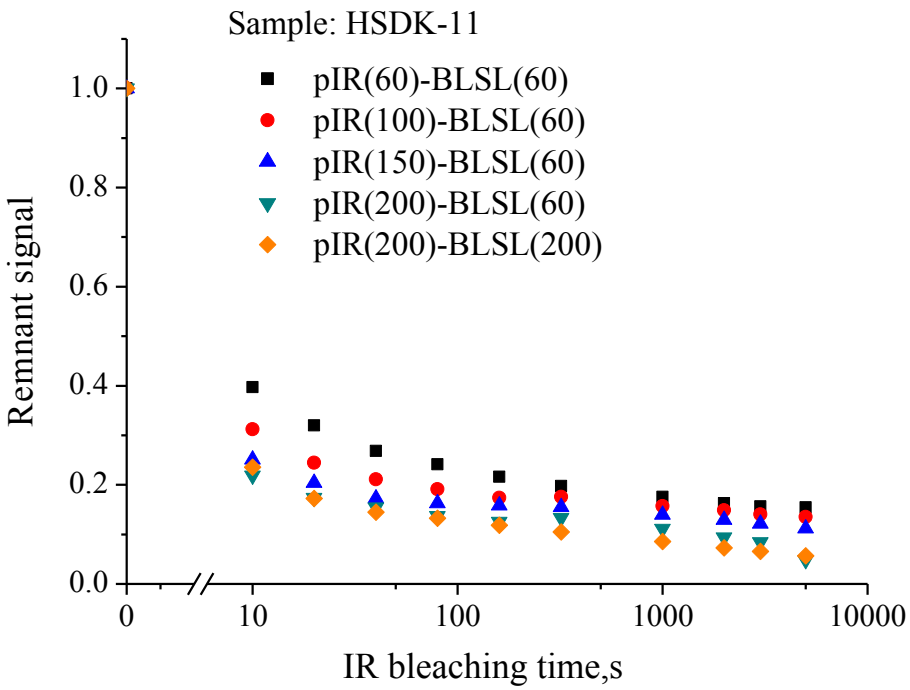
Sample: HSDK-11
pIR(60)-BLSL(60)
pIR(100)-BLSL(60)
pIR(150)-BLSL(60)
pIR(200)-BLSL(60)
pIR(200)-BLSL(200)
Remnant signal
1.0
0.8
0.6
0.4
0.2
0.0
0
10
100
1000
10000
IR bleaching time,s

682

683 Figure 2a

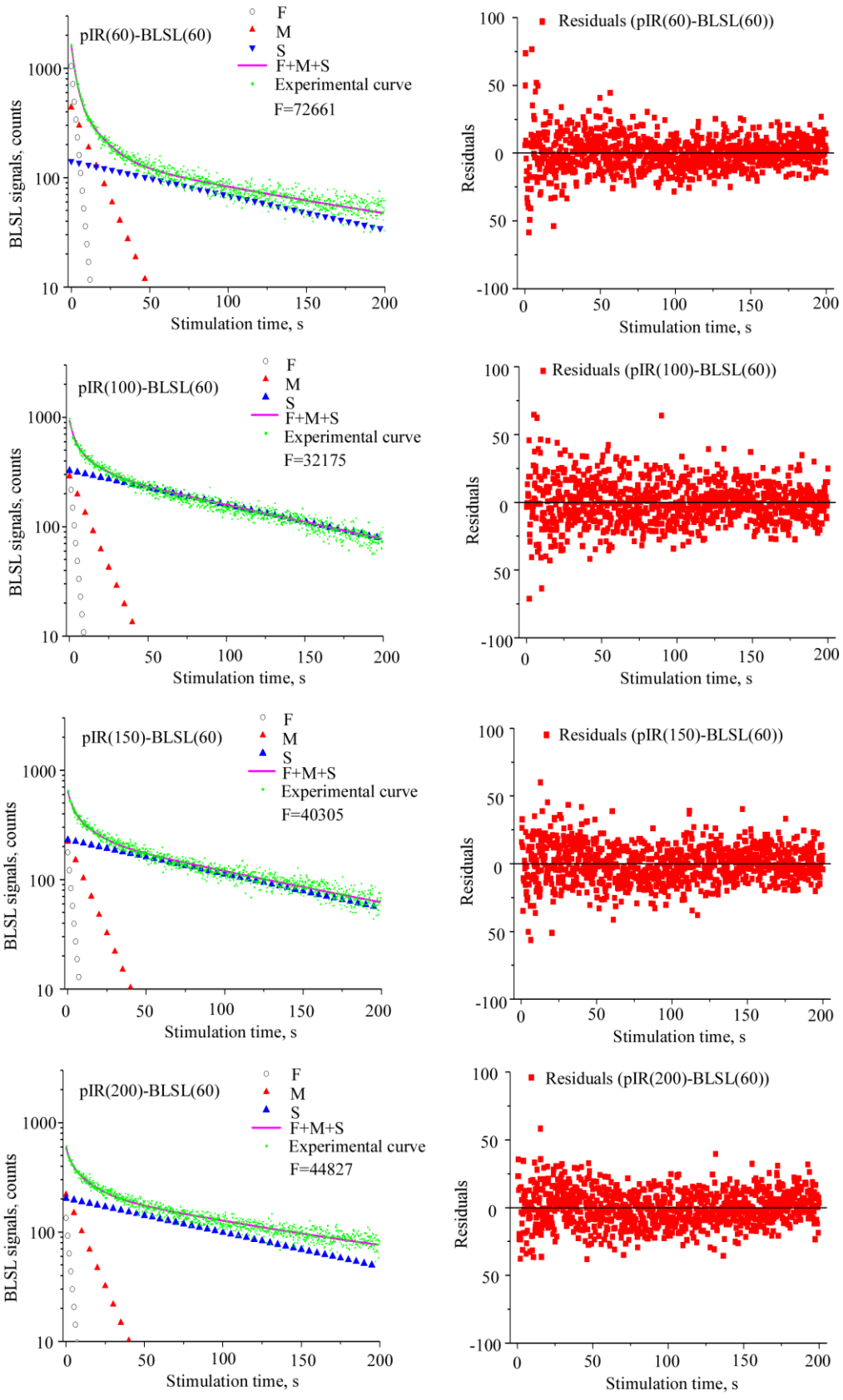

684

Figure 2b

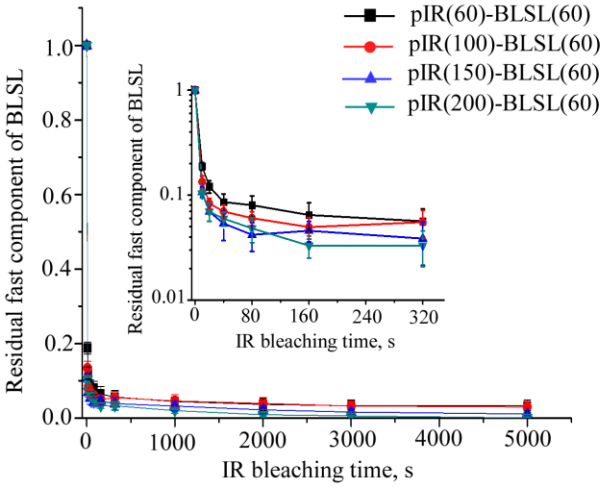
pIR(60)-BLSL(60)
pIR(100)-BLSL(60)
pIR(150)-BLSL(60)
pIR(200)-BLSL(60)
Residual fast component of BLSL
IR bleaching time, s

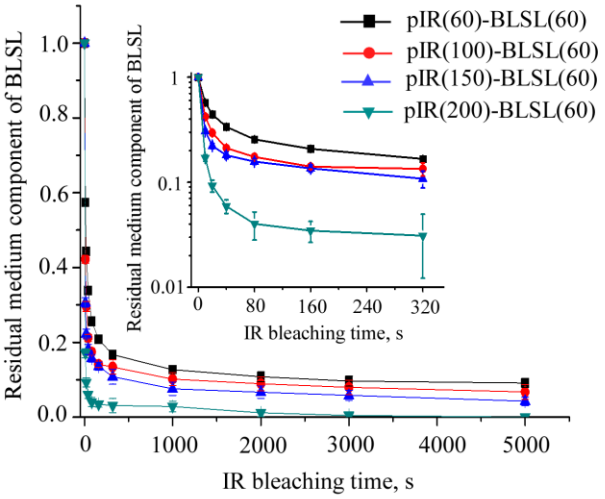
pIR(60)-BLSL(60)
pIR(100)-BLSL(60)
pIR(150)-BLSL(60)
pIR(200)-BLSL(60)
Residual medium component of BLSL
IR bleaching time, s

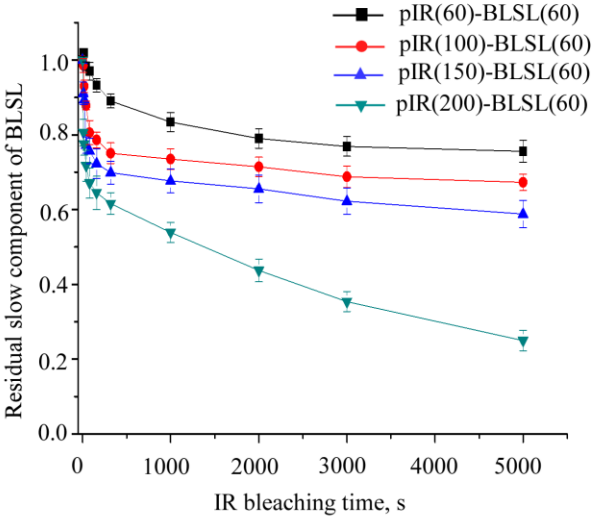
pIR(60)-BLSL(60)
pIR(100)-BLSL(60)
pIR(150)-BLSL(60)
pIR(200)-BLSL(60)
Residual slow component of BLSL
IR bleaching time, s

Figure 3

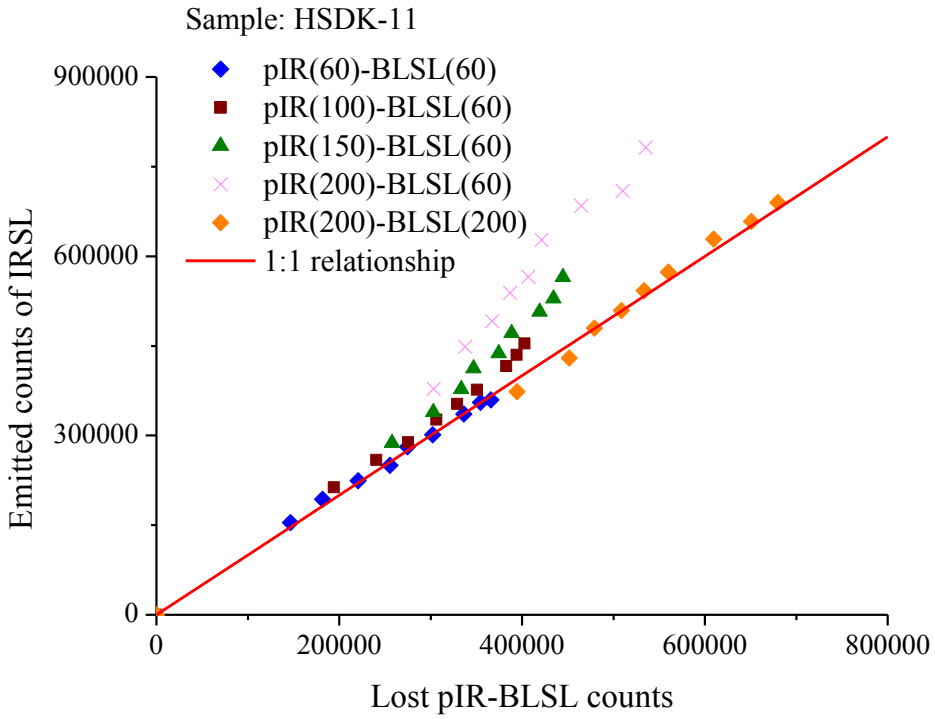
Sample: HSDK-11
pIR(60)-BLSL(60)
pIR(100)-BLSL(60)
pIR(150)-BLSL(60)
pIR(200)-BLSL(60)
pIR(200)-BLSL(200)
1:1 relationship
Emitted counts of IRSL
Lost pIR-BLSL counts
0
300000
600000
900000
0
200000
400000
600000
800000

Figure 4

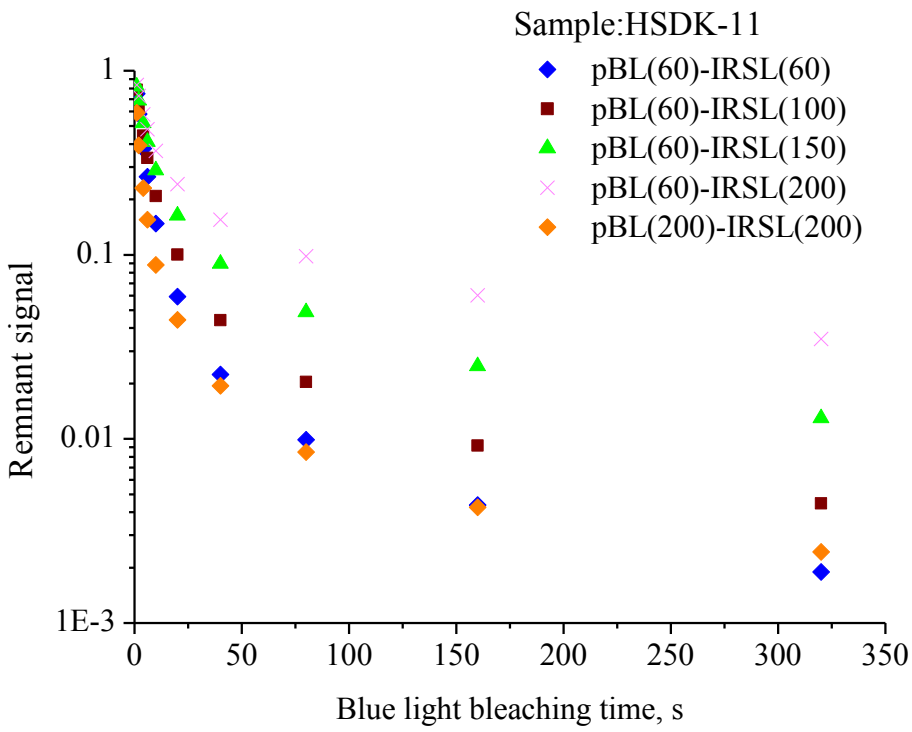
Sample:HSDK-11
pBL(60)-IRSL(60)
pBL(60)-IRSL(100)
pBL(60)-IRSL(150)
pBL(60)-IRSL(200)
pBL(200)-IRSL(200)
Remnant signal
1
0.1
0.01
1E-3
0
50
100
150
200
250
300
350
Blue light bleaching time, s

Figure 5

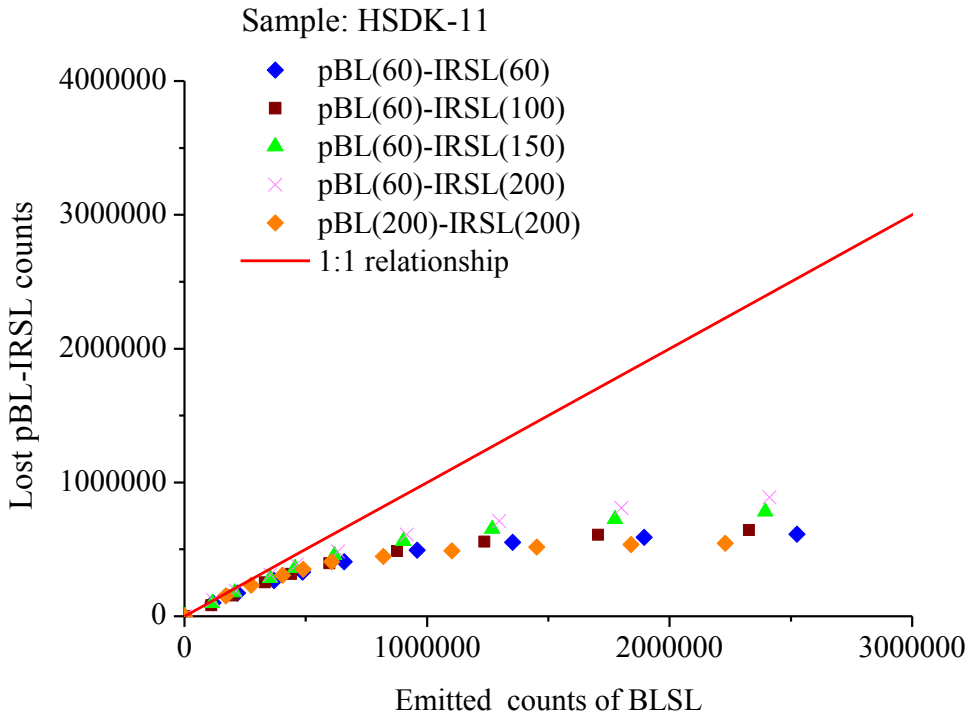
Sample: HSDK-11
pBL(60)-IRSL(60)
pBL(60)-IRSL(100)
pBL(60)-IRSL(150)
pBL(60)-IRSL(200)
pBL(200)-IRSL(200)
1:1 relationship
Lost pBL-IRSL counts
Emitted counts of BLSL
0
1000000
2000000
3000000
4000000

805

806 Figure 6

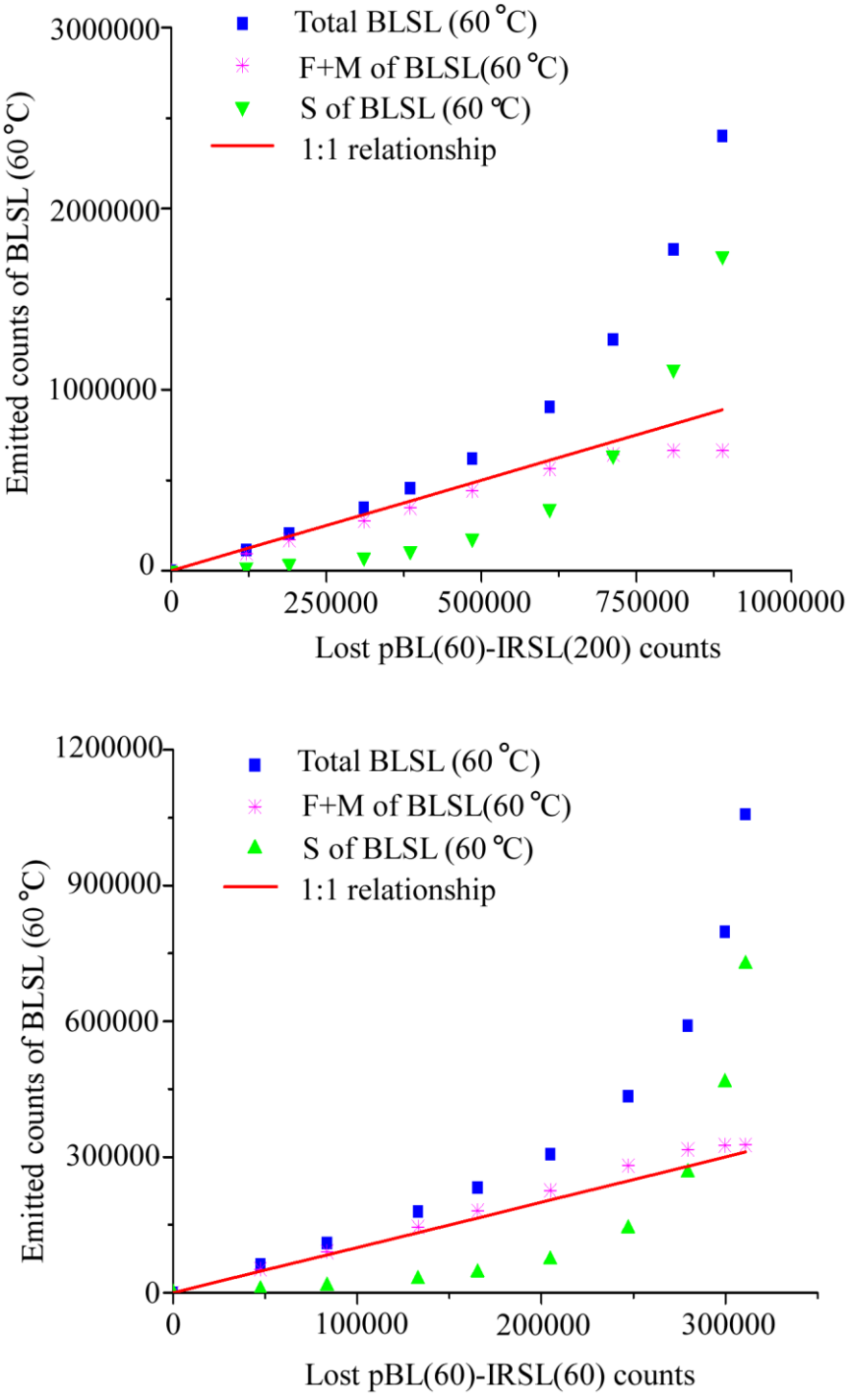

807

808

809

810

Figure 7

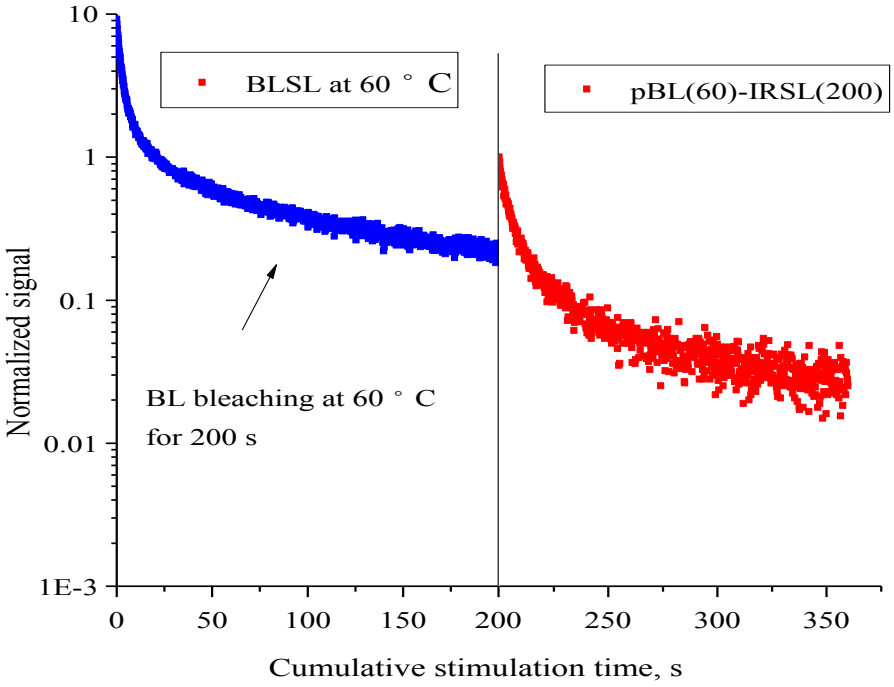
BLSL at 60 ° C
pBL(60)-IRSL(200)
BL bleaching at 60 ° C
for 200 s
Normalized signal
Cumulative stimulation time, s
10
1
0.1
0.01
1E-3
0
50
100
150
200
250
300
350

Figure 8

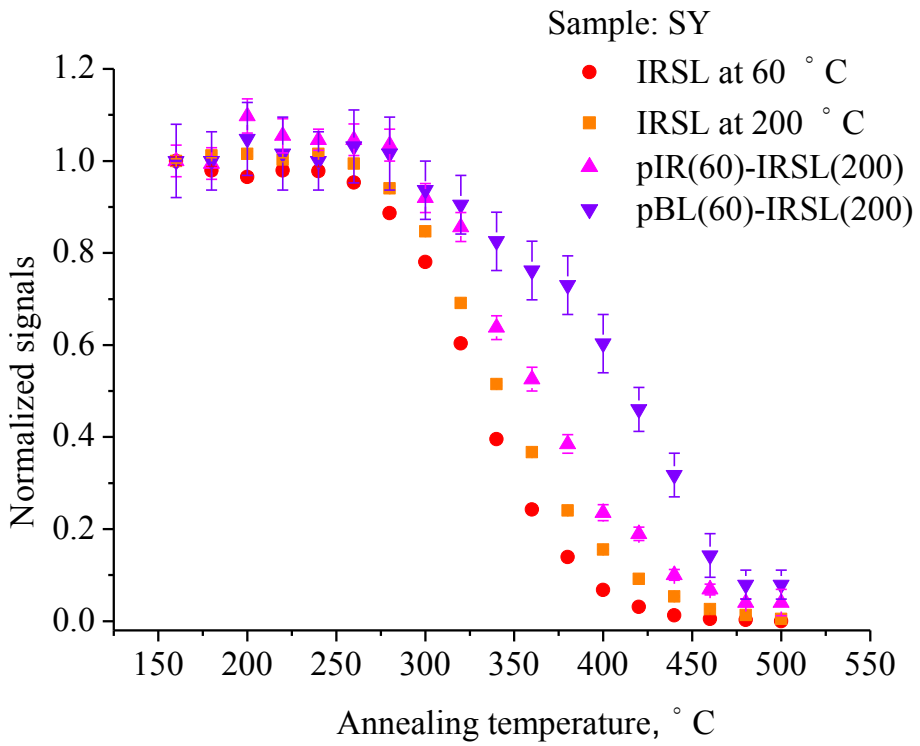
Sample: SY
IRSL at 60 ˚C
IRSL at 200 ˚C
pIR(60)-IRSL(200)
pBL(60)-IRSL(200)
Normalized signals
Annealing temperature, ˚C
0.0
0.2
0.4
0.6
0.8
1.0
1.2
150
200
250
300
350
400
450
500
550

Figure 9

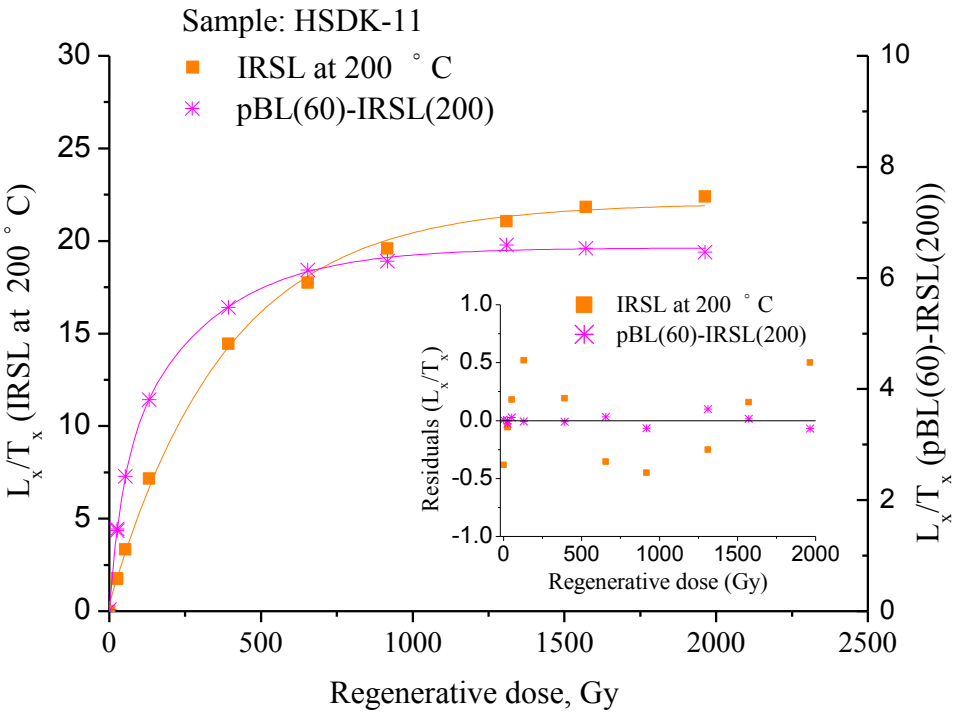
Sample: HSDK-11
IRSL at 200 ° C
pBL(60)-IRSL(200)
L_x/T_x (IRSL at 200 ° C)
L_x/T_x (pBL(60)-IRSL(200))
Regenerative dose, Gy
Residuals (L_x/T_x)
Regenerative dose (Gy)

865

866

867 Figure 10

868

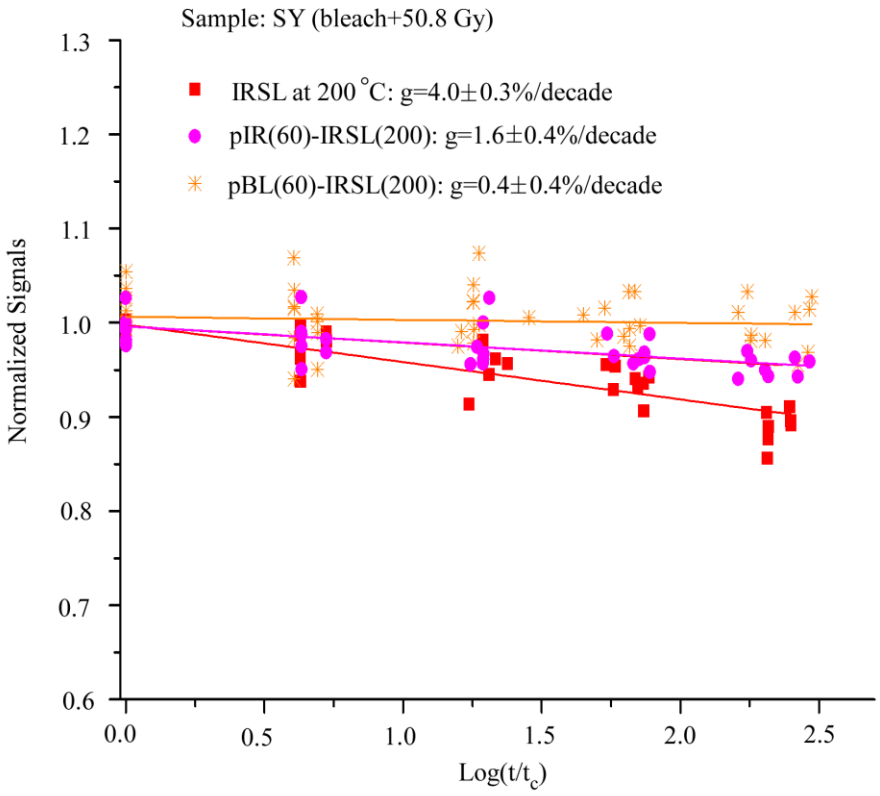

869

870

871

872

873

874

875

876

877

878

879

Table 1

Experimental procedures for the pIR(T_1)-BLSL(T_2) and pBL(T_2)-pIRSL(T_1) experiments. T_1 were set at 60,100, 150, 200 °C respectively, while T_2 were set at 60 and 200 °C.

	pIR(T_1)-BLSL(T_2)		pBL(T_2)-pIRSL(T_1)	
Step	Treatment	Observed	Treatment	Observed
(1)	Cut-heat to 500 °C		Cut-heat to 500 °C	
(2)	Regenerative dose (30.4 Gy)		Regenerative dose (30.4 Gy)	
(3)	Preheat to 280 °C for 10 s		Preheat to 280 °C for 10 s	
(4)	IR bleaching at T_1 for different time (0-5000 s)		BL bleaching at T_2 for different time (0-320 s)	
(5)	BLSL measurement at T_2 for 200 s	$L_{pIR\text{-}BLSL}$	IRSL measurement at T_1 for 160 s	$L_{pBL\text{-}IRSL}$
(6)	Test dose (15.2 Gy)		Test dose (15.2 Gy)	
(7)	Preheat to 280 °C for 10s		Preheat to 280 °C for 10s	
(8)	BLSL measurement at T_2 for 200 s	T_{BLSL}	IRSL measurement at T_1 for 160 s	T_{IRSL}
(9)	Return to step 1 and time for bleaching changes		Return to step 1 and time for bleaching changes	

Table 2

Pulse annealing procedures for the IRSL at 60 °C, the IRSL at 200 °C, the pIR(60)-IRSL(200) and the pBL(60)-IRSL(200). Note that the sequence of IRSL at 60 °C is steps 1, 2, 3, 4, 5a, 6, 7, 8a and 9, the sequence of IRSL at 200 °C is steps 1, 2, 3, 4, 5b, 6, 7, 8b and 9, the sequence of pIR(60)-IRSL(200) is steps 1, 2, 3, 3a, 4, 5b, 6, 7, 8b and 9 and the sequence of pBL(60)-IRSL(200) is steps 1, 2, 3, 3b, 4, 5b, 6, 7, 8b and 9.

Step	Treatment	Observed
(1)	Cut-heat to 500 °C	
(2)	Regenerative dose (30.4 Gy)	
(3)	Preheat to 280 °C for 10 s	
(3a)	IR bleaching at 60 °C for 200 s	
(3b)	BL bleaching at 60 °C for 200 s	
(4)	Cut-heat to T °C (160 °C -500 °C)	
(5a)	IRSL measurement at 60 °C for 160 s	$L_{(IRSL\ 60\ °C)}$
(5b)	IRSL measurement at 200 °C for 160 s	$L_{(IRSL\ 200\ °C)}$
(6)	Test dose (30.4 Gy)	
(7)	Preheat to 280 °C for 10 s	
(8a)	IRSL measurement at 60 °C for 160 s	$T_{(IRSL\ 60\ °C)}$
(8b)	IRSL measurement at 200 °C for 160 s	$T_{(IRSL\ 200\ °C)}$
(9)	Return to step 1 and T = T +20 °C	

*Unmarked Manuscript (clean version)
Click here to download Unmarked Manuscript (clean version): paper after second revision clean.docx Click here to view linked References

Further studies on the relationship between IRSL and BLSL at relatively high temperatures for potassium-feldspar from sediments

Zhijun Gong[a,b], Bo Li[a,c], Sheng-Hua Li[a,*]

[a] Department of Earth Sciences, The University of Hong Kong, Pokfulam Road, Hong Kong, China

[b] Key laboratory of Cenozoic Geology and Environment, Institute of Geology and Geophysics, Chinese Academy of Sciences, Beijing, China

[c] Centre for Archaeological Science, School of Earth and Environmental Sciences, University of Wollongong, Wollongong, NSW 2522, Australia

*Corresponding author: shli@hku.hk

Abstract:

In optical dating of potassium-feldspar, the luminescence signals can be stimulated by both infrared (IR) light and blue light (BL). To develop reliable dating methods using different stimulation light sources for feldspars, it is important to understand the sources of the traps associated with the infrared stimulated luminescence (IRSL) and blue light stimulated luminescence (BLSL) and their relationship. In this study, we explored the luminescence characteristics of IRSL and BLSL at different stimulation temperatures (from 60 °C to 200 °C) and their relationship based on five sets of experiments, i.e. post-IR BLSL, post-BL IRSL experiments, pulse annealing test, dose response test and laboratory fading rate test. Our results suggest that the luminescence characteristics of IRSL and BLSL and their relationship are dependent on stimulation temperature. For IR stimulation at a relatively high temperature of 200 °C, at least two components of IRSL signals are involved in the process. One component of IRSL signals can be easily bleached by BL stimulation at 60 °C, while the other is relatively hard to be bleached by BL stimulation at 60 °C. The two components have different luminescence properties, such as thermal stability, dose response and laboratory fading rate.

Keywords: K-feldspar, IRSL, BLSL, component

1. Introduction

Both quartz and potassium-rich feldspar (K-feldspar) have been widely used as natural dosimeters for optically stimulated luminescence (OSL) dating (Aitken, 1998). Compared with quartz OSL, the infrared stimulated luminescence (IRSL) signal from K-feldspar (Hütt et al., 1988) has advantages of much brighter luminescence signals and much higher dose saturation level, making feldspar as an attractive candidate for luminescene dating of the natural sedimentary samples. However, the usage of K-feldspar for dating has long been hindered by the anomalous fading of the trapped charges related to the IRSL signals (e.g. Spooner, 1994; Huntley and Lamonthe, 2001; Li and Li, 2008).

More recently, progress in understanding anomalous fading in feldspar has raised the prospect of isolating a non-fading component from the IRSL at relatively high temperatures (Thomsen et al., 2008; Li, 2010; Jain and Ankjærgaard, 2011; Li and Li, 2013). Correspondingly, a two-step post IR IRSL (pIRIR) protocol (Buylaert et al., 2009; Thiel et al., 2011) and a multi-elevated-temperature post-IR IRSL (MET-pIRIR) protocol (Li and Li, 2011a) have been proposed to overcome anomalous fading for dating K-feldspar from sediments, which offer the promising potential for extending the luminescence dating limit (Thiel et al., 2011; Li and Li, 2012; Li et al., 2013, However, the high temperature pIRIR signal (e.g. >200 °C) is found to be more to bleach than the IRSL signal measured at lower temperatures (Li and Li, 2011a; Buylaert et al., 2012; Murray et al., 2012), and it usually requires up to several hours even days of exposure to sunlight or a solar simulator to bleach the pIRIR signal down to a stable level (here the term “bleach” means to reduce the luminescence intensity by optical stimulation). For some samples, a significant non-bleachable (or residual) component in the pIRIR signals was left even after a prolonged bleaching period using solar simulator or sunlight (Buylaert et al., 2011; Lowick et al., 2012; Chen et al., 2013; Li et al., 2014b). These studies suggest that the IRSL signals recorded at relatively high temperature have different luminescence behavior compared with the IRSL signals at room temperature.

There have been several studies conducted to explore the relationship between

luminescence with IR stimulation and luminescence with visible wavelength light stimulation. It was demonstrated that the majority of green light stimulated luminescence (GLSL) can be bleached by prolonged IR light and an upper limit of ~ 90% GLSL was depleted as a result of IR bleaching at room temperature (Duller and Bøtter-Jensen, 1993; Galloway, 1994). Jain and Singhvi (2001) concluded that the blue-green (BG) stimulated luminescence measured at 125 °C is associated with at least two trap populations. One trap population is responsive to both IR stimulation and BG stimulation. Another trap population is only responsive to BG stimulation. Gong et al. (2012) conducted a study on the relationship between the infrared stimulated luminescence (IRSL) and blue light stimulated luminescence (BLSL) at 60 °C. They observed that most of the IRSL signals at 60 °C can be bleached by BL at 60 °C, while the BLSL signals at 60 °C can only be partially bleached by IR at 60 °C. The sources for the IRSL at 60 °C are mainly associated with the fast and medium components of the BLSL at 60 °C.

In this study, in order to better understand the sources of the traps associated with the IRSL and BLSL, we further explore the relationship between IRSL and BLSL using K-feldspar from two aeolian sand samples. The luminescence properties, in terms of thermal stability, dose response and laboratory fading rate, are also examined for the different IRSL components at a relatively high temperature of 200 °C.

2. Samples and equipment

Two aeolian sand samples (HSDK-11 and SY) from the Hunshandake desert in northeast China were used in this study. Both samples have been investigated in previous studies (Li et al., 2002; Gong et al., 2013). The samples are from the same environmental settings of the same region and have similar luminescence behaviors, so the experimental results obtained from them should be comparable. The samples were treated with 10 % hydrochloric acid (HCl) and 10 % hydrogen peroxide (H_2O_2) to remove carbonate and organic matter, respectively, in subdued red light in the

Luminescence Dating Laboratory, the University of Hong Kong. Grains of 150-180 μm in diameter were obtained by dry sieving. The K-feldspar grains were separated with heavy liquids (2.58 $g \cdot cm^{-3}$) and then etched for 40 min with diluted (10 %) hydrofluoric acid (HF) to clean the grains. HCl (10 %) was used again to dissolve any contaminating fluorides after etching before final rinsing and drying. K-feldspar grains were prepared by mounting the grains in a monolayer, on a 9.8 mm diameter aluminum disc with "Silkospay" silicone oil.

The luminescence measurements of the sample HSDK-11 were carried out with an automated Risø TL-DA-15 reader equipped with an IR LED array (880 nm, FWHM 40 nm) and a blue LED array (470 nm, FWHM 20 nm) in the Luminescence Dating Laboratory, the University of Hong Kong. The IR and BL stimulations deliver ~135 $mW \cdot cm^{-2}$ and ~50 $mW \cdot cm^{-2}$ at the sample position, respectively (Bøtter-Jensen et al., 2003). To keep our results comparable with those from Gong et al. (2012), 90% of the full power was used for stimulation in this study. Irradiations were carried out within the reader using a $^{90}Sr/^{90}Y$ beta source which delivered a dose rate of 0.0761 $Gy \cdot s^{-1}$ to K-feldspar on aluminum discs. The IRSL and the BLSL signals were both detected after passing through 7.5-mm-thick U-340 filters, which mainly pass light from 290 nm to 370 nm with peak transmission at ~340 nm (Li et al., 2007b). The experimental work on the other sample SY was performed in the Luminescence Dating Laboratory, Institute of Geology and Geophysics, Chinese Academy of Sciences. The luminescence measurements of the sample SY were carried out with an automated Risø TL/OSL reader (TL/OSL-DA-15) using the similar equipment setting. The $^{90}Sr/^{90}Y$ beta source in the equipment delivered a dose rate of 0.0837 $Gy \cdot s^{-1}$ to K-feldspar on aluminum discs.

3. Experimental details and results

3.1 The relationship between the IRSL and the BLSL at different stimulation temperatures

Two sets of experiments, namely post-IR BLSL (pIR-BLSL) and post-blue light IRSL (pBL-IRSL), are conducted to investigate the relationship between the IRSL and the BLSL at different stimulation temperatures. For simplification, we describe the stimulation temperatures used in the prior IR and post-IR BLSL as pIR(T_1)-BLSL(T_2), where T_1 is the stimulation temperature used in the prior IR measurement and T_2 is the temperature used in post-IR BLSL measurement.

3.1.1 pIR-BLSL experiments

The pIR-BLSL experiments were carried out using the procedure listed in Table 1. Four aliquots of of K-feldspar grains HSDK-11 were firstly heated to 500 °C and then given a dose of 30.4 Gy. These aliquots were subsequently preheat at 280 °C for 10 s and then bleached using IR stimulation at a temperature of T_1 for different periods ranging from 0 to 5000 s. The pIR-BLSL signal (L_x) was then measured at a temperature of T_2. After that, a test dose of 15.2 Gy was applied and the induced BLSL signal (T_x) was measured following the same preheat to monitor sensitivity change for L_x. The signals for both L_x and T_x were calculated from the integrated photon counts in the first 1 s of stimulation, with subtraction of the instrumental background signal. The experiments are conducted at a set of different temperature combinations, i.e. pIR(60)-BLSL(60), pIR(100)-BLSL(60), pIR(150)-BLSL(60), pIR(200)-BLSL(60) and pIR(200)-BLSL(200), respectively.

The IR bleaching effects on the pIR-BLSL signal for different periods of time are shown in Fig. 1. It is observed that the IR bleaching at higher temperatures can deplete the BLSL at 60 °C at a faster rate than IR stimulation at lower temperatures. The BLSL at 60 °C was bleached to about 5 % of the initial intensity after IR bleaching at 200 °C for 5000 s. In comparison, the BLSL at 60 °C was bleached to about 15 % of the initial intensity after IR bleaching at 60 °C for 5000 s. If we increase the stimulation temperature in BLSL from 60 to 200 °C, i.e. pIR(200)-BLSL (200), the IR stimulation at 200 °C can bleach the most of the traps associated with the BLSL at 200 °C and only 6 % of the initial intensity of the BLSL at 200 °C was

remaining after IR bleaching at 200 °C for 5000 s (Fig. 1). The results suggest that both the BLSL measured at 60 °C and the BLSL at 200 °C can only be partially bleached by prolonged (up to 5000 s) IR stimulation even at a relatively high temperature (i.e. 200 °C).

In our previous study (Gong et al., 2012), it was found that the BLSL signals measured at 60 °C for the K-feldspar from sample HSDK-11 can be described using three first-order exponential components, which are termed as fast (F), medium (M) and slow (S) components. Gong et al. (2012) demonstrated that the sources for the IRSL at 60 °C are mainly associated with the fast and medium components of the BLSL at 60 °C. To further demonstrate the relationship between IRSL signal at relatively high temperatures and BLSL at 60 °C, the residual BLSL at 60 °C after IR bleaching for different time from 0 s to 5000 s were then fitted using three OSL components. It is found that the pIR-BLSL signals can be well described by the three exponential functions (all $R^2 > 0.96$). The relative ratios of the decay rates of the components of BLSL at 60 °C, i.e. b_f/b_m and b_m/b_s, are calculated at 4.87±0.14 and 10.69±0.41, respectively (here the parameters of b_f, b_m and b_s refer to the decay rate of the fast, medium and slow components of BLSL at 60 °C, respectively). It is noted that the assumption of that the BLSL process is first-order may not be true. However, this will not influence our conclusion because it is the relationship between the different parts of BLSL (represented by the fast, medium and slow components) and IRSL that is crucial for our study, rather than whether these components are first-order or not. We, however, acknowledge that there may be some uncertainty associated with the fitting and some results demonstrated by Fig. 2 and Fig. 6 might be partially influenced if these components are not first-order.

Fig. 2a illustrates four representative pIR-BLSL signals, which are fitted into three components. The results of IR bleaching for the fast, medium and slow component of BLSL at 60 °C are shown in Fig. 2b. It is observed that the IR stimulation at 200 °C for 5000 s can deplete 99 % of the fast component, ~99 % of the medium component but only ~38 % of the slow component for the BLSL at 60 °C, while IR stimulation at 60 °C for 5000 s can only deplete ~97 % of fast component, ~91 % of medium

component and ~12 % of slow component, respectively, for the BLSL at 60 °C. These results indicate that IRSL obtained at 200 °C involves more traps associated with hard-to-bleach components (i.e. the medium and slow components) of BLSL at 60 °C than does the IR stimulation at 60 °C. The results are consistent with previous studies that the IRSL signals at high temperatures (e.g. >200 °C) are relatively harder to bleach than the IRSL at 60 °C (Buylaert et al., 2011; Li and Li, 2011a; Chen et al., 2013).

The relationship between the IRSL and BLSL at different temperatures is further studied by investigating the relationship between the emitted light counts from the IRSL and the corresponding lost counts obtained from the pIR(T_1)-BLSL(T_2) experiments (T_1= 60, 100, 150, 200 °C; T_2= 60, 200 °C). This is similar to the method applied to study the relation between IRSL and thermoluminescence (TL) by Duller (1995). In Fig. 3, we plot the emitted counts from the IRSL, against the corresponding lost counts of the pIR-BLSL as a result of IR bleaching. It is observed that, if the stimulation temperature for IR and BL was identical in both cases (i.e. pIR(60)-BLSL(60) and pIR(200)-BLSL(200)), the emitted counts of the IRSL have a nearly 1:1 relationship with the corresponding lost counts in the pIR-BLSL. However, in the case of T_1>T_2, the emitted counts of the IRSL are larger than the corresponding lost counts in pIR-BLSL, indicating that the relationship between BLSL and IRSL is dependent on the stimulation temperature. It is to be noted that such a relationship between IRSL and BLSL is not influenced by the interference of isothermal TL, because the preheat at 280 °C for 10 s is sufficient to remove any isothermal TL at 200 °C. One straightforward explanation for the temperature dependency of the relationship is that at least two components are involved in the IRSL at the relatively high temperature (such as the IRSL at 200 °C). One component is responsive to the BL at 60 °C. The other is hard to reach by BL at 60 °C, but can be accessed at higher temperatures. The results further support fact that the IRSL signals at relatively high temperatures are relatively harder to bleach than the IRSL at 60 °C (e.g. Chen et al., 2013).

3.1.2 pBL-IRSL experiments

The effects of BL bleaching at 60 °C and 200 °C on the IRSL signals at different temperatures (60, 100, 150 and 200 °C) are investigated using pBL-IRSL experiments (see the procedures listed in Table 1). The experiments conducted are pBL(60)-IRSL(60), pBL(60)-IRSL(100), pBL(60)-IRSL(150), pBL(60)-IRSL(200) and pBL(200)-IRSL(200), respectively. Four aliquots of K-feldspar grains of HSDK-11 were firstly heated to 500 °C to remove any residual signals and then given the same irradiation dose of 30.4 Gy. These aliquots were then held at 280 °C for 10 s. They were subsequently bleached with BL at 60, 200 °C for different periods from 0 to 320 s before IRSL measurements. After that, the IRSL sensitivity was monitored and measured following a test dose of 15.2 Gy and preheat at 280 °C for 10 s.

The remnant IRSL at different temperatures (50, 100, 150 200 °C) as a result of BL bleaching at 60, 200 °C for different periods of time are shown in Fig. 4. It is demonstrated that the IRSL at 60 °C can be bleached to a negligible level (~0.2 %) by BL stimulation at 60 °C for 320 s, while 3.5 % of the initial IRSL at 200 °C still remains after BL bleaching at 60 °C for 320 s. These results indicate that, compared with the IRSL at 60 °C, the IRSL at 200 °C involves more traps that are harder to bleach by BL at 60 °C. However, the IRSL at 200 °C can be bleached to a negligible level (~0.2 %) by BL stimulation at 200 °C for 320 s. In addition, the decay rates in the pBL(200)-IRSL (200) and the pBL(60)-IRSL(60) are very similar and they are calculated at 0.23 ±0.02 s^{-1} and 0.21 ±0.01 s^{-1}, respectively. These results further suggest that the relationship between the IRSL and the BLSL is dependent on stimulation temperature.

Further investigation is made on the relationship between the emitted counts from the BLSL and the corresponding lost counts from pBL(T_1)-IRSL(T_2) (T_1= 60, 200 °C; T_2= 60, 100, 150, 200 °C) (Fig. 5). It is observed that the emitted counts from the BLSL measured both at 60 °C and at 200 °C are significantly larger than the corresponding lost counts from pBL(T_1)-IRSL(T_2). These results indicate that BL can

240 access much more traps than IR stimulation. Only part of traps associated with the
241 BLSL at 60 °C and at 200 °C is accessible by IR stimulation, which is similar to the
242 results of IRSL observed at 60 °C (Gong et al, 2012). It is also demonstrated that
243 relationship between emitted BLSL counts and lost counts of pBL-IRSL changes as
244 the stimulation temperature changes.

245 To further demonstrate the relationship between different OSL components of the
246 BLSL signal at 60 °C and the IRSL signals at relatively high temperatures, the emitted
247 light counts from different OSL components of the BLSL signal at 60 °C are
248 compared with the corresponding lost counts from the pBL(60)-IRSL(200) and
249 pBL(60)-IRSL(60) as a result of BL bleaching at 60 °C for different periods. We plot
250 the emitted counts from the various OSL components of the BLSL at 60 °C, against
251 the lost counts of IRSL at 60 °C and IRSL at 200 °C as a result of BL bleaching in Fig.
252 6. It is observed that the lost counts in pBL(60)-IRSL(200) are larger than the sum of
253 the emitted light counts of the fast and medium components of BLSL at 60 °C, while
254 the lost counts in pBL(60)-IRSL(60) have a nearly 1:1 relationship with the sum of
255 the emitted light counts of the fast and medium components of BLSL at 60 °C. These
256 results indicate that the IRSL signals at 200 °C are involved with not only the fast and
257 medium components of BLSL at 60 °C, but also some other OSL components (e.g.
258 slower components of BLSL at 60 °C). In contrast, there is a close relationship
259 between IRSL at 60 °C and the fast and medium components of BLSL at 60 °C (Gong
260 et al., 2012). The results are consistent with the observations in previous section 3.1.1.

261 In summary, the results from the pIR-BLSL and pBL-IRSL bleaching experiments
262 suggest that the relationship between IRSL and BLSL is dependent on stimulation
263 temperature. At least two components of traps are involved in the IRSL measured at
264 elevated temperatures (e.g., 200 °C). One component can be easily bleached by BL at
265 60 °C, and the other of the IRSL is relatively harder to access by BL at 60 °C. The
266 results show that the IRSL signals at relatively high temperatures are harder to be
267 bleached than the IRSL at room temperature.

268

269 3.2 Luminescence properties of IRSL at relatively high temperature

The luminescence characteristics of the IRSL at 200 °C, the pIR(60)-IRSL(200) and the pBL(60)-IRSL(200), including thermal stability, dose response and laboratory fading rate, were further investigated. In both the pIR(60)-IRSL(200) and the pBL(60)-IRSL(200) experiments, the IR and BL bleaching time was both fixed at 200 s.

3.2.1 Thermal stability study

The thermal stability studies are carried out using the pulse annealing test (Table 2) (Li et al., 1997; Li and Tso, 1997). The tests were conducted for the IRSL at 60 °C, the IRSL at 200 °C, the pIR(60)-IRSL(200) and the pBL(60)-IRSL(200), respectively. An aliquot of K-feldspar of SY was firstly heated to 500 °C and then given an irradiation dose of 30.4 Gy. After that, it was preheated at 280 °C for 10 s and then heated to a temperature at T °C before the remaining IRSL was measured at 60 °C for 160 s. The sensitivity change was monitored by measuring the IRSL signal at 60 °C from a test dose of 30.4 Gy. The same preheat condition (280 °C for 10 s) was applied for the test dose IRSL measurement. This cycle was repeated by increasing the annealing temperature (T) from 160 °C to 500 °C in steps of 20 °C. The similar pulse annealing test procedures were also conducted for the IRSL at 200 °C, the pIR(60)-IRSL(200) and the pBL(60)-IRSL(200) (Table 2). The heating rate for all these pulse annealing experiments was 3 °C·s^{-1}.

The typical decay curve of the pBL(60)-IRSL(200) signal is shown in Fig. 7. The results of the pulse annealing test of the IRSL at 60 °C, the IRSL at 200 °C, the pIR(60)-IRSL(200) and the pBL(60)-IRSL(200) are shown in Fig. 8. It is observed that the thermal stability of the IRSL at 200 °C is relatively more stable than that of the IRSL at 60 °C. Li and Li (2011b; 2013) also observed the different thermal stabilities among the IRSL at different stimulation temperatures. In addition, it is found that both pIR(60)-IRSL(200) and pBL(60)-IRSL(200) is more thermally stable than IRSL at 200 °C. The results suggest that at least two components are involved in

300 the IRSL at 200 °C and the components have significantly different thermal stability.
301 Both IR at 60 °C and BL at 60 °C can remove the thermally relatively unstable
302 component of IRSL 200 °C. It is interesting to be noted that the pBL(60)-IRSL(200)
303 is significantly more thermally stable than pIR(60)-IRSL(200), indicating that the BL
304 at 60 °C is more efficient than IR at 60 °C to reduce thermally unstable component in
305 the IRSL at 200 °C.
306
307 3.2.2 Dose response curves
308
309 Different shapes of dose response curve (DRC) may provide an indication of
310 different origins of different luminescence signals (Gong et al., 2012). Here we
311 compare the DRC of the IRSL at 200 °C from K-feldspar with that of the
312 pBL(60)-IRSL(200). Regenerative doses ranging from 0 to 1950 Gy were employed
313 in a single aliquot regeneration (SAR) protocol for the IRSL at 200 °C. A test dose of
314 52 Gy was applied and the test dose signal (T_x) was measured to monitor and correct
315 for sensitivity change. A recycle dose at 26 Gy was used and the recycling ratios all
316 fall within the range of 1.0 ± 0.05 for the sample. The preheat temperature (held at
317 280 °C for 10 s) was the same for regeneration and test dose measurements. A
318 cut-heat to 500 °C was used between each of the SAR cycles to clean the residual
319 signals from the previous cycle. The IRSL signals L_x and T_x were calculated from the
320 integrated photon counts in the first 1 s of stimulation, with subtraction of a
321 background signal derived from the last 10 s of the 160 s stimulation. For construction
322 the DRC of the pBL(60)-IRSL(200), a similar SAR procedure was applied, except
323 that a BL bleaching at 60 °C for 200 s was added before each IRSL measurement for
324 both the regenerative and test dose measurements. The dose response curves for the
325 two signals are shown in Fig. 9. It is found that the pBL(60)-IRSL(200) signal have a
326 different dose saturation level with the IRSL at 200 °C.
327 If the two dose response curves are fitted with double saturation exponential
328 function (equation 1),

$$I = I_0 + I_a(1-\exp(-D/D_{0,a})) + I_b(1-\exp(-D/D_{0,b})) \quad (1)$$

The dose saturation level of two D_0 ($D_{0,a}$ and $D_{0,b}$) parameters are 42.9±5.8 Gy and 289.7±22.4 Gy for the pBL(60)-IRSL(200) signal, while the values of two D_0 ($D_{0,a}$ and $D_{0,b}$) parameters of the IRSL at 200 °C are significantly higher at 214.6±9.9 Gy and 806.1±69.6 Gy, respectively. The results indicate that at least two components are involved in the IRSL at elevated temperature. One group is easy to bleach by BL at 60 °C and they have a higher dose saturation level, while the other group is hard to bleach by BL at 60 °C and they have a lower dose saturation level.

3.2.3 Laboratory fading test

Anomalous fading was observed for both IRSL and BLSL signals in previous studies (e.g. Thomsen et al., 2008). Here we studied the laboratory fading rates for the IRSL at 200 °C, the pIR(60)-IRSL(200) and the pBL(60)-IRSL(200) signals. In measurement of the IRSL at 200 °C, six aliquots of SY were heated to 500 °C to remove any residual signals (similar to a hot-bleach between SAR cycles). Then these aliquots were given 50.8 Gy and immediately preheated at 280 °C for 10 s. The sensitivity corrected signals were then measured after delays of different periods. For the test dose, 12.7 Gy was given and the same preheat condition was applied. The IRSL signals $L_{(x)}$ and $T_{(x)}$ were calculated from the integrated photon counts in the first 1 s of stimulation, with subtraction of a background signal derived from the last 10 s of the 160 s stimulation. The first measurement of the IRSL at 200 °C signal took place at a time t_c= 562 s after the mid-point of the irradiation time. A similar measurement procedure was adopted for measuring the fading rate for the pIR(60)-IRSL(200) and pBL(60)-IRSL(200) signals. For the pIR(60)-IRSL(200) signal, an IR bleaching at 60 °C for 200 s was added before the IRSL measurement at 200 °C for both the regenerative and test dose measurements. The first measurement of the pIR(60)-IRSL(200) signal took place at a time t_c= 669 s after the mid-point of

357 the irradiation time. For the pBL(60)-IRSL(200) signal, a BL bleaching at 60 °C for
358 200 s was added before the IRSL measurement at 200 °C for both the regenerative
359 and test dose measurements. The first measurement of the pBL(60)-IRSL(200) signal
360 took place at a time t_c= 669 s after the mid-point of the irradiation time. The decay of
361 the IRSL at 200 °C, the pIR(60)-IRSL(200) and the pBL(60)-IRSL(200) signals after
362 normalization as a function of storage time is shown in Fig 10. The corresponding
363 anomalous fading rates (g-value) are calculated based on the data sets and are also
364 shown in Fig. 10. It is observed that the IRSL at 200 °C, the pIR(60)-IRSL(200) and
365 the pBL(60)-IRSL(200) have significantly different laboratory fading rates. The g
366 value for the IRSL at 200 °C was detected at 4.0±0.3 %/decade, the g value of the
367 pIR(60)-IRSL(200) was at 1.6±0.4 %/decade and the pBL(60)-IRSL(200) was 0.4±
368 0.4 %/decade. This result indicates that there are at least two components for the IRSL
369 at 200 °C. One component is easy to bleach by IR at 60 °C and BL at 60 °C and it has
370 higher laboratory fading rate, while the other is hard to bleach by IR at 60 °C and BL
371 at 60 °C and it has a significantly lower fading rate.
372
373 ## 4. Discussion
374 The sources and process of the traps associated with IRSL from feldspar are
375 important for developing reliable dating methods. Different models have been
376 proposed to explain the various luminescence behaviors of feldspars. A single trap
377 model has been proposed recently to explain the luminescence characteristics for
378 feldspar (e.g., Jain and Ankjærgaard, 2011; Anderson et al., 2012), while a multi-trap
379 model is suggested alternatively by others (e.g., Duller and Bøtter-Jensen, 1993; Li
380 and Li, 2011; Thomsen et al., 2011; Li et al., 2014). These studies were based on their
381 own experimental designs with limited experimental conditions and the explanations
382 are based on different assumptions, so a unique interpretation cannot be reached. It is
383 hoped that the study of the relationship between BLSL and IRSL could be helpful for
384 understanding the source and process of IRSL, because, unlike IRSL process, BLSL is
385 expected to be a simpler and delocalized process due to the higher photon energy of

BL (~2.64 eV) compared to the main IRSL trap depth (~2.5 eV) (e.g. Baril and Huntley, 2003; Kars et al., 2013). Based on our results, we are in favor of the multiple-trap model to explain the experimental data obtained in this study, which cannot be well explained using a simple single-trap model. The pieces of evidence are given as follows:

(1) If we assume that IRSL at 200 °C and 60 °C originate the same traps and then both signals should be depleted by BL at a similar rate, because BL have energy high enough to evict the trapped electron to the conduction band and then the electron can randomly recombine with both close and distant holes. In Fig. 4, it is clearly shown that, compared with the IRSL at 60 °C, the IRSL at 200 °C is bleached at the significantly slower rate by BL at 60 °C, suggesting that IRSL signals at 200 °C are involved with traps which are very hard to bleach by BL at 60 °C. This could be due to either that the hard-to-bleach component has a deeper trap depth (>2.5 eV) or that the component has a different photoionization cross-section, which both indicate a different trap from the easy to bleach component.

(2) During the pIR(60)-BLSL(60) experiments, the emitted counts of the IRSL have a nearly 1:1 relationship with the corresponding lost counts in the pIR-BLSL. However, this is not the case for the pIR(200)-BLSL(60) (Fig. 3). This indicates that IRSL at elevated temperature can access more traps that are more difficult to bleach by BL at 60 °C.

(3) The pBL(60)-IRSL(200) and IRSL signals at 200 °C have very different luminescence properties, such as thermal stability, dose response and fading rate. Since BL have energy high enough to evict the trapped electron to the conduction band, the electron will randomly recombine with close or distant holes after excitation. Hence, BL will cause not only recombination of spatially close electron-hole pairs, but also recombination of distant electron-hole pairs. As a result, BL bleaching should not change the relative proportions between close and distant electron-hole pairs. Correspondingly, it is expected that the pBL-IRSL should have a similar thermal stability as IRSL, and the pIR-IRSL should have a higher thermal stability than pBL-IRSL. Our results, however, showed that the pBL(60)-IRSL(200) is significantly

more thermally stable than both the IRSL at 200 °C and pIR(60)-IRSL(200) (Fig. 8), which cannot be explained by the single-trap model. Similarly, a similar fading rate should be expected for the IRSL(200) and pBL(60)-IRSL(200) signals based on a single-trap model. For our samples, the g values for the IRSL at 200 °C are greatly reduced after the BL bleaching at 60 °C for 200 s (Fig. 10). It is interesting to be noted that the laboratory fading rate of pBL(60)-IRSL(200) is significantly lower than that of pIR(60)-IRSL(200), suggesting that the BL at 60 °C is more efficiently than the IR at 60 °C to remove spatially close electron-hole pairs (easy-to-fade), which cannot be explained by a single trap model.

Based on the above arguments, we think that a single trap model is not sufficient to explain all the luminescence phenomena in feldspar. In the future, it is maybe helpful to use time-resolved optically stimulated luminescence (TR-OSL) technique to further study the luminescence behaviors of K-feldspar (e.g. Chithambo and Galloway, 2001).

Another outcome of our study is that we first demonstrate that the pBL(60)-IRSL(200) has a high thermal stability and a negligible fading rate, which opens the potential of using this signal in sediments dating without the corrections for anomalous fading. A potential advantage of using pBL(60)-IRSL(200) is that blue bleaching at 60 °C can eliminate the contribution of quartz grains to IRSL at elevated temperatures (Fan et al., 2009). Quartz grains can coexist with K-feldspar after heavy liquid separation. The IRSL of quartz at elevated temperatures can be effectively bleached by blue light at low temperatures, but not by infrared. Further tests on the applicability in dating are required to confirm the suitability of using the pBL-IRSL at relatively high temperatures.

5. Conclusions

From the pIR-BLSL and pBL-IRSL bleaching experiments, it is concluded that the relationship between IRSL and BLSL is dependent on the stimulation temperature. If stimulation temperatures for the IRSL increase from 60 to 200 °C, at least two

components are associated with the IRSL at 200 °C. One component is easy to bleach by BL at 60 °C, and the other relative hard to bleach by BL at 60 °C. The two components of the IRSL at 200 °C have significantly different luminescence properties, in terms of thermal stability, dose saturation level and laboratory fading rates.

Acknowledgments

This study was financially supported by the grants to Sheng-Hua Li from the Research Grant Council of the Hong Kong Special Administrative Region, China (Project nos. 7028/08P and 7033/12P). The authors are grateful to the two anonymous reviewers for providing valuable comments and suggestions on the manuscript.

476

477 Reference

478 Adamiec, G., 2005. OSL decay curves—relationship between single- and
479 multiple-grain aliquots. Radiation Measurements 39, 63-75.

480 Aitken, M.J., 1998. An Introduction to Optical Dating. Oxford Unversity Press,
481 Oxford.

482 Andersen, M.T., Jain, M., Tidemand-Lichtenberg, P., 2012. Red-IR stimulated
483 luminescence in K-feldspar: Single or multiple trap origin? Journal of Applied
484 Physics 112, 043507, DOI 10.1063/1.4745018.

485 Bøtter-Jensen, L., Andersen, C.E., Duller, G.A.T., Murray, A.S., 2003. Developments
486 in radiation, stimulation and observation facilities in luminescence measurements.
487 Radiation Measurements 37, 535-541.

488 Baril, M. R., and Huntley, D. J., 2003, Optical excitation spectra of trapped electrons
489 in irradiated feldspars: Journal of Physics-Condensed Matter, v. 15, no. 46, p.
490 8011-8027.

491 Buylaert, J.P., Jain, M., Murray, A.S., Thomsen, K.J., Thiel, C., and Sohbati, R., 2012,
492 A robust feldspar luminescence dating method for Middle and Late Pleistocene
493 sediments. Boreas 41, 435-451.

494 Buylaert, J.P., Murray, A.S., Thomsen, K.J., Jain, M., 2009. Testing the potential of an
495 elevated temperature IRSL signal from K-feldspar. Radiation Measurements 44,
496 560-565.

497 Buylaert, J.P., Thiel, C., Murray, A., Vandenberghe, D.G., Yi, S., Lu, H., 2011. IRSL
498 and post-IR IRSL residual doses recorded in modern dust samples from the
499 Chinese Loess Plateau. Geochronometria 38, 432-440.

500 Chen, Y., Li, S.-H., Li, B., 2013. Residual doses and sensitivity change of post IR
501 IRSL signals from potassium feldspar under different bleaching conditions.
502 Geochronometria 40, 229-238.

503 Chithambo, M.L., Galloway, R.B., 2001. On the slow component of luminescence
504 stimulated from quartz by pulsed blue light-emitting diodes. Nuclear Instruments
505 and Methods in Physics Research Section B: Beam Interactions with Materials

and Atoms 183, 358-368.

Duller, G.A.T., 1995. Infrared bleaching of the thermoluminescence of four feldspars. Journal of Physics D: Applied Physics 28, 1244.

Duller, G.A.T., Bøtter-Jensen, L., 1993. Luminescence from Potassium Feldspars Stimulated by Infrared and Green Light. Radiation Protection Dosimetry 47, 683-688.

Fan, A.C., Li, S.-H., Li, B., 2009. Characteristics of quartz infrared stimulated luminescence (IRSL) at elevated temperatures. Radiation Measurements 44, 434-438.

Galloway, R.B., 1994. Comparison of the green- and infrared-stimulated luminescence of feldspar. Radiation Measurements 23, 617-620.

Gong, Z., Li, B., Li, S.-H., 2012. Study of the relationship between infrared stimulated luminescence and blue light stimulated luminescence for potassium-feldspar from sediments. Radiation Measurements 47, 841-845.

Gong, Z., Li, S.-H., Sun, J., Xue, L., 2013. Environmental changes in Hunshandake (Otindag) sandy land revealed by optical dating and multi-proxy study of dune sands. Journal of Asian Earth Sciences 76, 30-36.

Hütt, G., Jaek, I., Tchonka, J., 1988. Optical Dating: K-Feldspars Optical Response Stimulation Spectra. Quaternary Science Reviews 7, 381-385.

Huntley, D.J., Lamothe, M., 2001. Ubiquity of anomalous fading in K-feldspars and the measurement and correction for it in optical dating. Canadian Journal of Earth Sciences 38, 1093-1106.

Jain, M., Ankjærgaard, C., 2011. Towards a non-fading signal in feldspar: Insight into charge transport and tunnelling from time-resolved optically stimulated luminescence. Radiation Measurements 46, 292-309.

Jain, M., Singhvi, A.K., 2001. Limits to depletion of blue-green light stimulated luminescence in feldspars: implications for quartz dating. Radiation Measurements 33, 883-892.

Kars, R.H., et al., 2013. On the trap depth of the IR-sensitive trap in Na- and K-feldspar. Radiation Measurements 59, 103-113.

536 Li, B., 2010. The relationship between thermal activation energy, infrared stimulated
537 luminescence and anomalous fading of K-feldspars. Radiation Measurements 45,
538 757-763.
539 Li, B., Jacobs, Z., Roberts, R.G., Li, S.-H., 2013. Extending the age limit of
540 luminescence dating using the dose-dependent sensitivity of MET-pIRIR signals
541 from K-feldspar. Quaternary Geochronology 17, 55-67.
542 Li, B., Jacobs, Z., Roberts, R., Li, S.-H., 2014b, Review and assessment of the
543 potential of post-IR IRSL dating methods to circumvent the problem of anomalous
544 fading in feldspar luminescence. Geochronometria, 41, 178-201.
545 Li, B., Li, S.-H., 2008. Investigations of the dose-dependent anomalous fading rate of
546 feldspar from sediments. Journal of Physics D-Applied Physics 41, 225502.
547 Li, B., Li, S.-H., 2011a. Luminescence dating of K-feldspar from sediments: A
548 protocol without anomalous fading correction. Quaternary Geochronology 6,
549 468-479.
550 Li, B., Li, S.-H., 2011b. Thermal stability of infrared stimulated luminescence of
551 sedimentary K- feldspar. Radiation Measurements 46, 29-36.
552 Li, B., Li, S.-H., 2012. Luminescence dating of Chinese loess beyond 130 ka using
553 the non-fading signal from K-feldspar. Quaternary Geochronology 10, 24-31.
554 Li, B., Li, S.-H., 2013. The effect of band-tail states on the thermal stability of the
555 infrared stimulated luminescence from K-feldspar. Journal of Luminescence 136,
556 5-10.
557 Li, B., Li, S.-H., Wintle, A.G., Zhao, H., 2007a. Isochron measurements of naturally
558 irradiated K- feldspar grains. Radiation Measurements 42, 1315-1327.
559 Li, B., Roberts, R.G., Jacobs, Z., Li, S.-H., 2014a. A single-aliquot luminescence
560 dating procedure for K-feldspar based on the dose-dependent MET-pIRIR signal
561 sensitivity. Quaternary Geochronology 20, 51-64.
562 Li, S.-H., Chen, Y.Y., Li, B., Sun, J.M., Yang, L.R., 2007b. OSL dating of sediments
563 from desert in northern China. Quaternary Geochronology 2, 23-28.
564 Li, S.-H., Sun, J.M., Zhao, H., 2002. Optical dating of dune sands in the northeastern
565 deserts of China. Palaeogeography Palaeoclimatology Palaeoecology 181,

419-429.

Li, S.-H., Tso, M.Y.W., 1997. Lifetime determination of OSL signals from potassium feldspar. Radiation Measurements 27, 119-121.

Li, S.-H., Tso, M.Y.W., Wong, N.W.L., 1997. Parameters of OSL traps determined with various linear heating rates. Radiation Measurements 27, 43-47.

Lowick, S.E., Trauerstein, M., and Preusser, F., 2012, Testing the application of post IR-IRSL dating to fine grain waterlain sediments. Quaternary Geochronology 8, 33-40.

Murray, A.S., Thomsen, K.J., Masuda, N., Buylaert, J.P., and Jain, M., 2012, Identifying well-bleached quartz using the different bleaching rates of quartz and feldspar luminescence signals: Radiation Measurements 47, 688-695.

Spooner, N.A., 1994. The anomalous fading of infrared-stimulated luminescence from feldspars. Radiation Measurements 23, 625-632.

Thiel, C., Buylaert, J.-P., Murray, A., Terhorst, B., Hofer, I., Tsukamoto, S., Frechen, M., 2011. Luminescence dating of the Stratzing loess profile (Austria) - Testing the potential of an elevated temperature post-IR IRSL protocol. Quaternary International 234, 23-31.

Thomsen, K.J., Murray, A.S., Jain, M., 2011. Stability of IRSL signals from sedimentary K-feldspar samples. Geochronometria 38, 1-13.

Thomsen, K.J., Murray, A.S., Jain, M., Bøtter-Jensen, L., 2008. Laboratory fading rates of various luminescence signals from feldspar-rich sediment extracts. Radiation Measurements 43, 1474-1486.

593 Figure captions

594

595 Figure 1: Remnant BLSL measured at 60 °C and 200 °C after IR bleaching at
596 different temperature for different times. The temperatures for IR bleaching were set
597 at 60, 100, 150 and 200 °C, respectively.

598

599 Figure 2: (a) four representative pIR-BLSL signals, which are then deconvoluted into
600 three components. For each of the fitting, the F-statistics are provided and they are all
601 significantly larger than $F_{0.01}$ (e.g. Adamiec, 2005). The corresponding residuals are
602 shown at the right. (b) The residual fast, medium and slow components of BLSL at
603 60 °C after IR bleaching for different time from 0 s to 5000 s. To better demonstrate
604 the data, the residual fast and medium components of BLSL at 60 °C after IR
605 bleaching for different time from 0 s to 320 s were further shown in the insets, while
606 the y-axis in the insets is on the logarithmic scale. The data were from sample
607 HSDK-11 and the fast, medium and slow components of BLSL at 60 °C were fitted
608 with the decay rates of 0.375 ± 0.004 s^{-1}, 0.077 ± 0.002 s^{-1} and 0.0072 ± 0.0002 s^{-1},
609 respectively, the same as Gong et al. (2012).

610

611 Figure 3: The relationship between emitted counts of the IRSL and the corresponding
612 lost counts of pIR(T_1)-BLSL(T_2) as a result of IR bleaching for different time. T_1= 60,
613 100, 150, 200 °C, T_2= 60, 200 °C respectively.

614

615 Figure 4: Remnant IRSL after blue light bleaching at 60 °C and 200 °C for different
616 times. The temperatures for IR stimulations were set at 60, 100, 150 and 200 °C,
617 respectively.

618

619 Figure 5: The relationship between emitted counts of the BLSL and the corresponding
620 lost counts of pBL(T_1)-IRSL(T_2) as a result of blue light bleaching for different time.
621 T_1= 60, 200 °C, T_2= 60, 100, 150, 200 °C, respectively.

Figure 6: The relationship between emitted counts of OSL components of BLSL at 60 °C and the lost counts of pBL(60)-IRSL(200) and pBL(60)-IRSL(60) as a result of blue light bleaching at 60 °C for different times. F+M: The sum of fast and medium components of the BLSL at 60 °C; S: slow component of the BLSL at 60 °C. The data were from sample HSDK-11.

Figure 7: The typical decay curves of the pBL(60)-IRSL(200) from sample HSDK-11. All the signals were normalized using the initial intensity of the pBL(60)-IRSL(200).

Figure 8: Pulse annealing curves based on the IRSL signal at 60 °C, the IRSL signal at 200 °C, pIR(60)-IRSL(200) and the pBL(60)-IRSL(200) signal; In the pIR(60)-IRSL(200) and pBL(60)-IRSL(200) experiments, the previous IR stimulation and BL stimulation at 60 °C are both at 200 s. The heating rate was 3 $°C \cdot s^{-1}$.

Figure 9: Dose response curves of the IRSL signal at 200 °C and the pBL(60)-IRSL(200) signal. The two dose response curves could be fitted well by the double saturation exponential function (R^2>0.99; residuals are shown in the inset).

Figure 10: Anomalous fading tests for IRSL signal at 200 °C, the pIR(60)-IRSL(200) and the pBL(60)-IRSL(200) signal using six aliquots from sample SY as a function of delayed period (t).

Figure 1

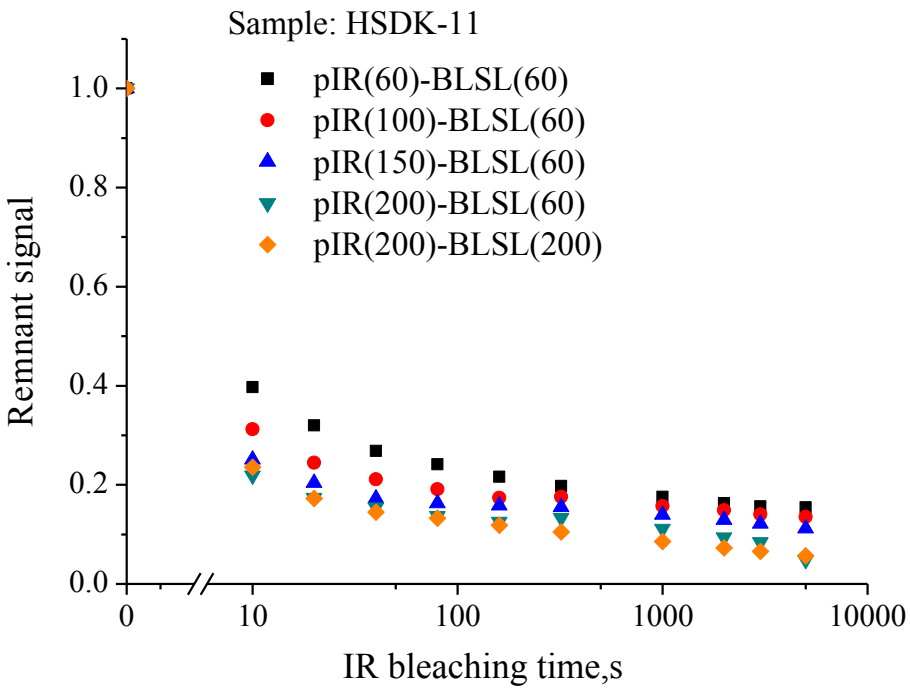
Sample: HSDK-11
pIR(60)-BLSL(60)
pIR(100)-BLSL(60)
pIR(150)-BLSL(60)
pIR(200)-BLSL(60)
pIR(200)-BLSL(200)
Remnant signal
1.0
0.8
0.6
0.4
0.2
0.0
0
10
100
1000
10000
IR bleaching time,s

682

683 Figure 2a

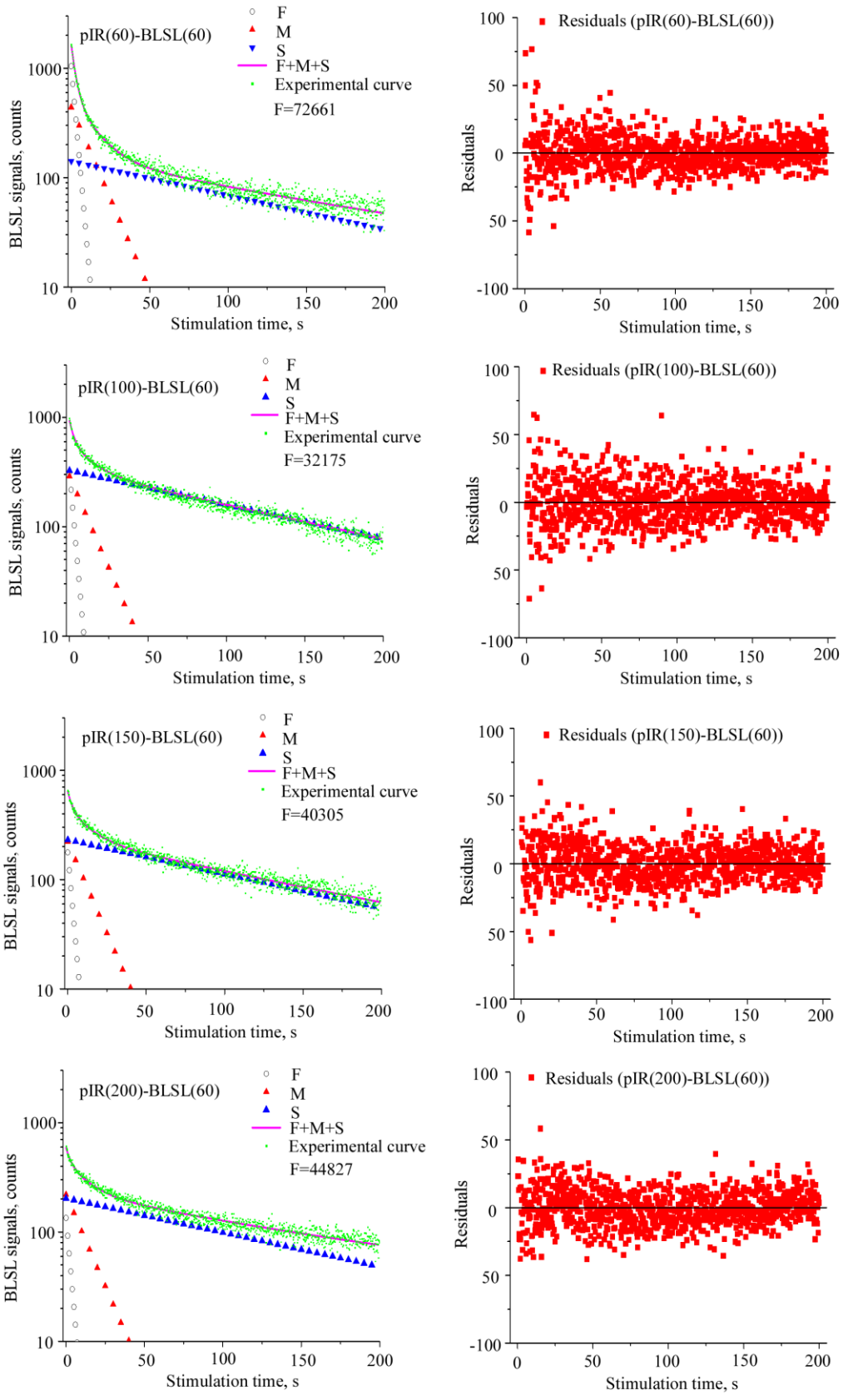

684

Figure 2b

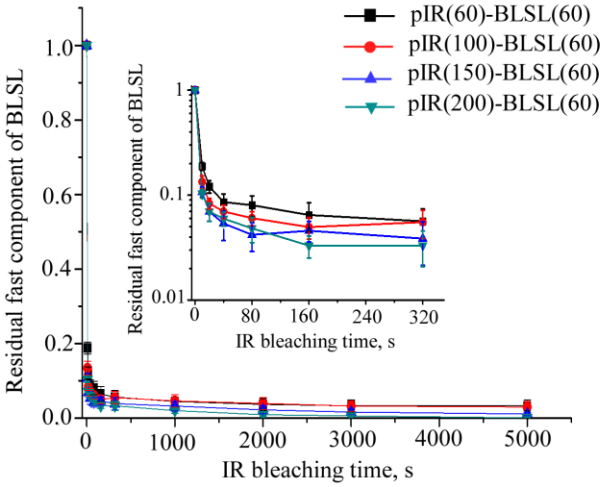
pIR(60)-BLSL(60)
pIR(100)-BLSL(60)
pIR(150)-BLSL(60)
pIR(200)-BLSL(60)
Residual fast component of BLSL
IR bleaching time, s

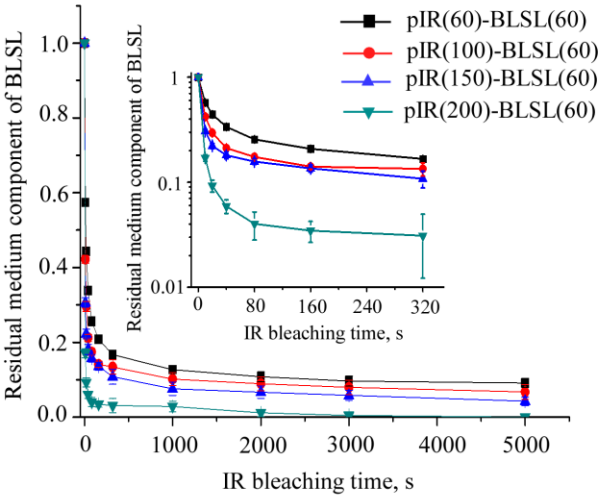
pIR(60)-BLSL(60)
pIR(100)-BLSL(60)
pIR(150)-BLSL(60)
pIR(200)-BLSL(60)
Residual medium component of BLSL
IR bleaching time, s

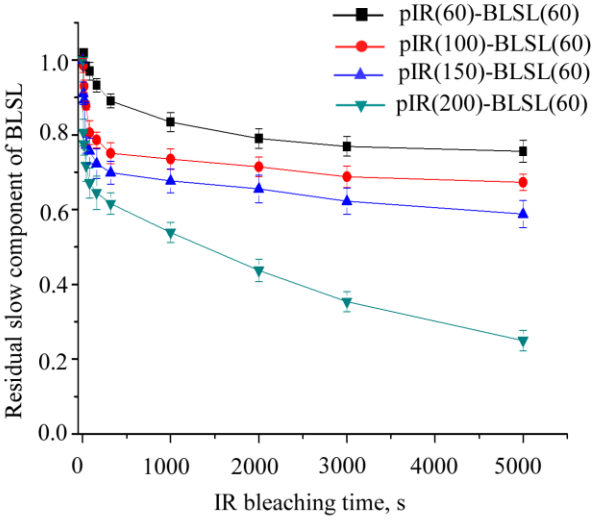
pIR(60)-BLSL(60)
pIR(100)-BLSL(60)
pIR(150)-BLSL(60)
pIR(200)-BLSL(60)
Residual slow component of BLSL
IR bleaching time, s

Figure 3

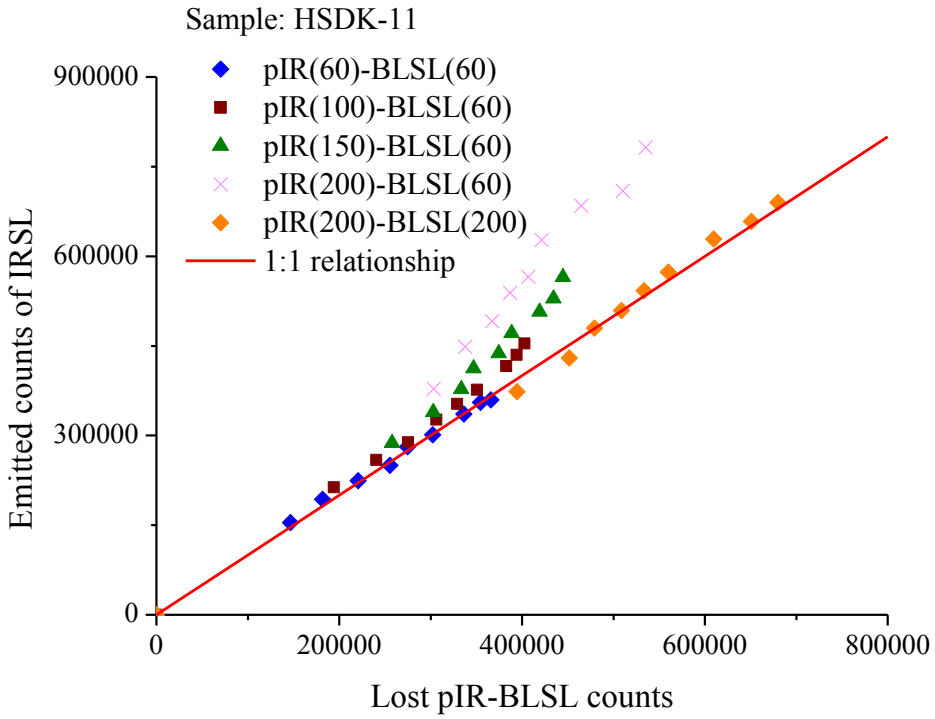
Sample: HSDK-11
pIR(60)-BLSL(60)
pIR(100)-BLSL(60)
pIR(150)-BLSL(60)
pIR(200)-BLSL(60)
pIR(200)-BLSL(200)
1:1 relationship
Emitted counts of IRSL
Lost pIR-BLSL counts
0
300000
600000
900000
0
200000
400000
600000
800000

Figure 4

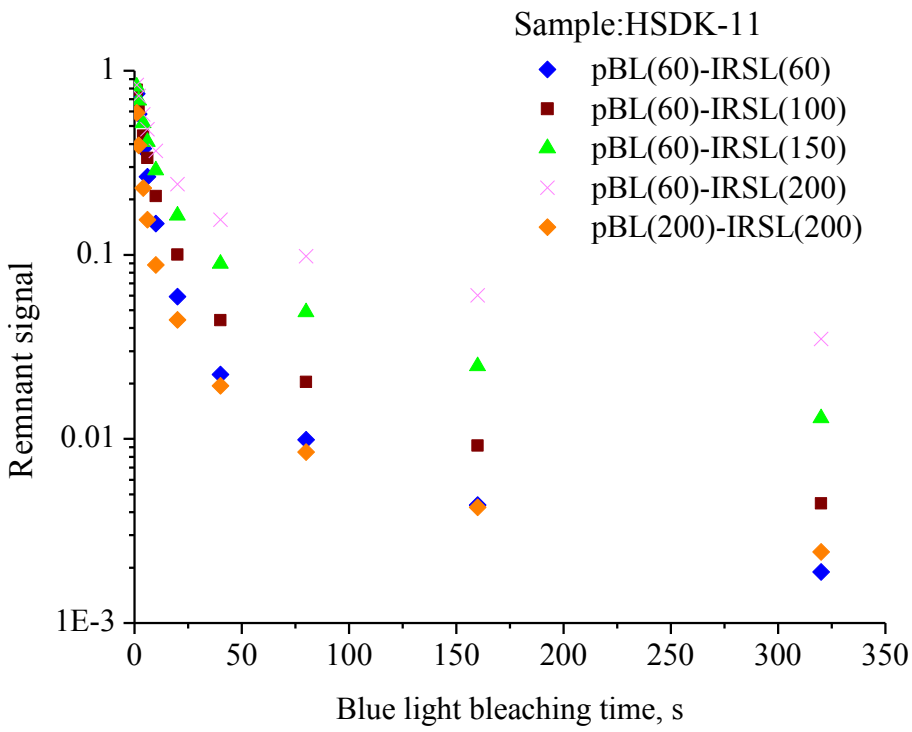
Sample:HSDK-11
pBL(60)-IRSL(60)
pBL(60)-IRSL(100)
pBL(60)-IRSL(150)
pBL(60)-IRSL(200)
pBL(200)-IRSL(200)
Remnant signal
1
0.1
0.01
1E-3
0
50
100
150
200
250
300
350
Blue light bleaching time, s

Figure 5

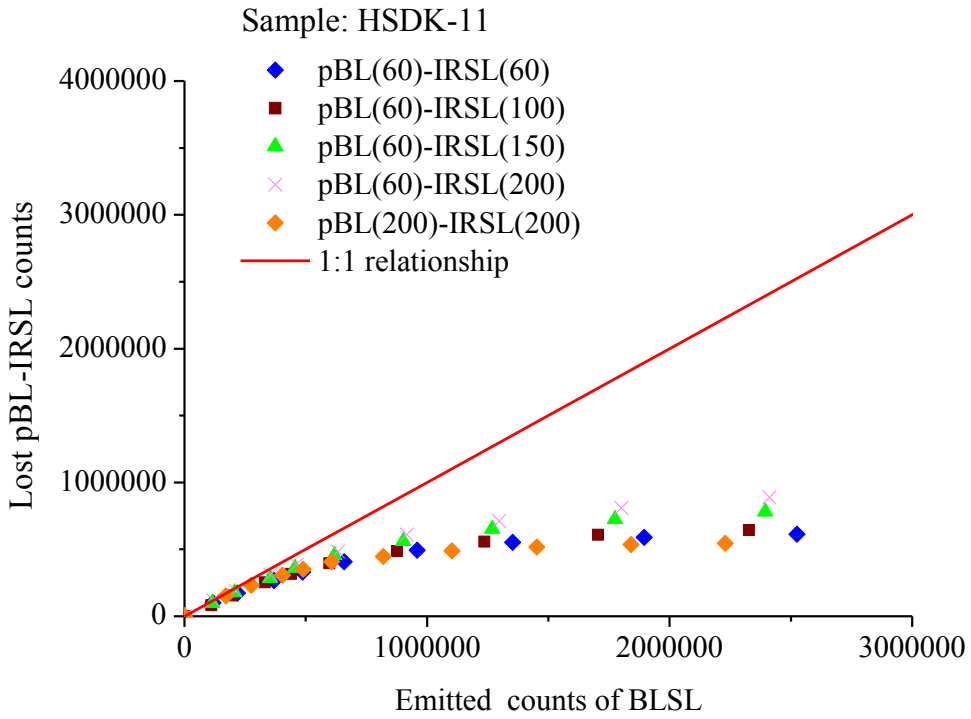
Sample: HSDK-11
pBL(60)-IRSL(60)
pBL(60)-IRSL(100)
pBL(60)-IRSL(150)
pBL(60)-IRSL(200)
pBL(200)-IRSL(200)
1:1 relationship
Lost pBL-IRSL counts
Emitted counts of BLSL
0
1000000
2000000
3000000
4000000

805

806 Figure 6

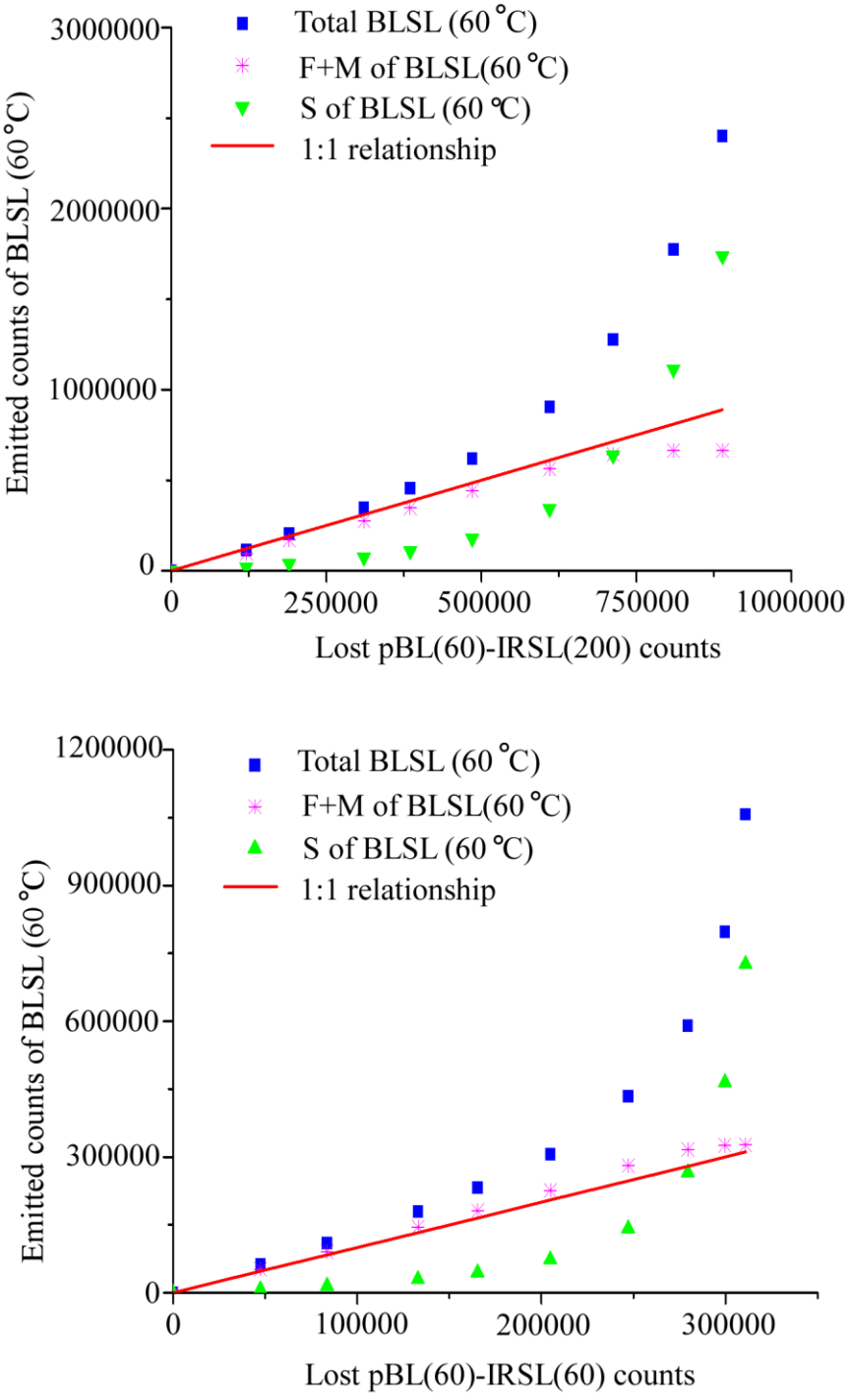

807

808

809

810

Figure 7

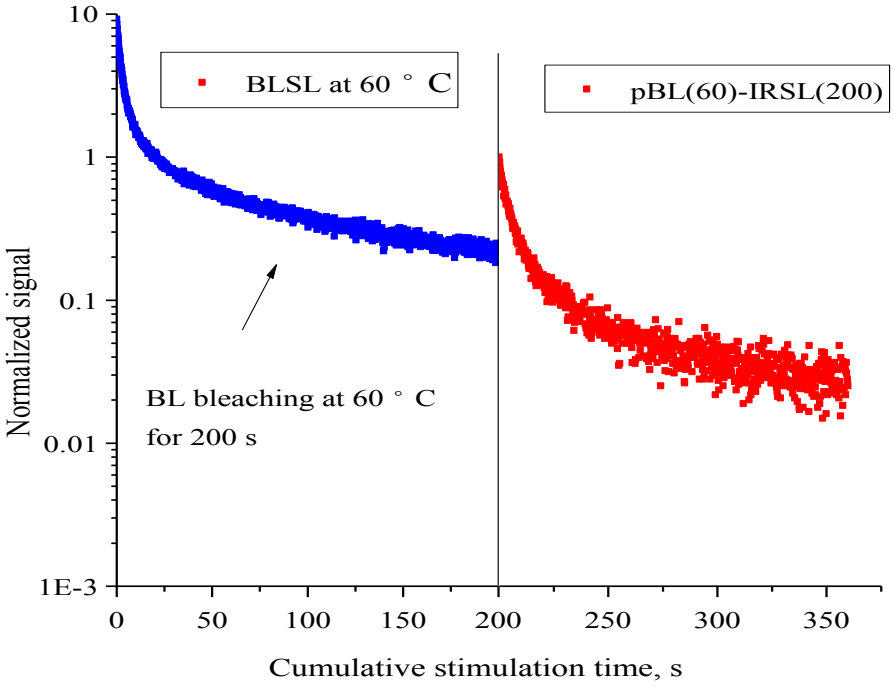
BLSL at 60 ° C
pBL(60)-IRSL(200)
BL bleaching at 60 ° C
for 200 s
Normalized signal
Cumulative stimulation time, s
10
1
0.1
0.01
1E-3
0
50
100
150
200
250
300
350

Figure 8

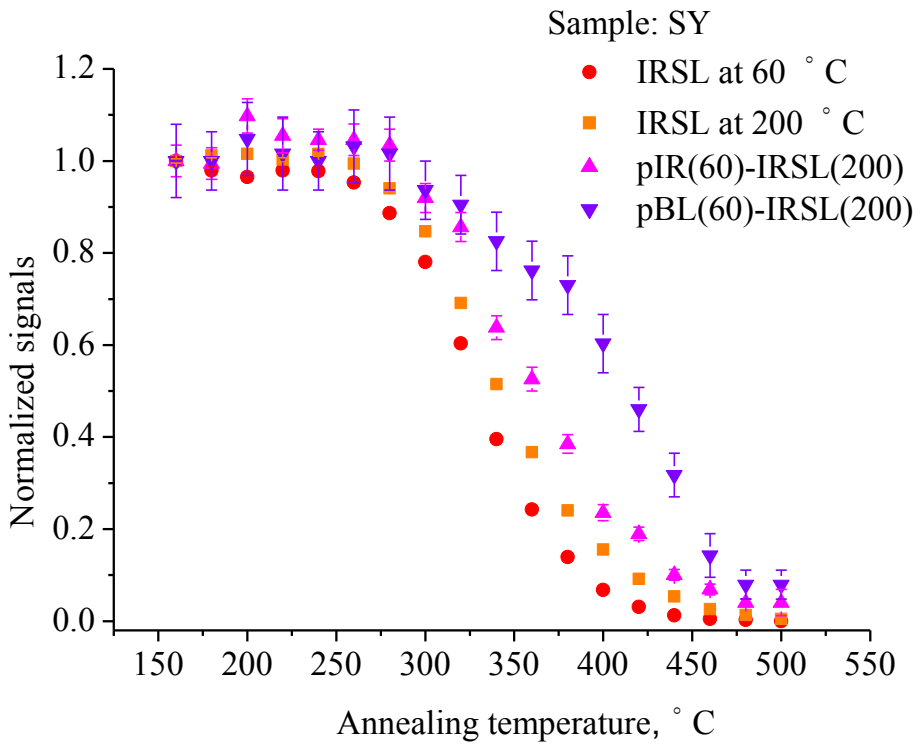
Sample: SY
IRSL at 60 ˚C
IRSL at 200 ˚C
pIR(60)-IRSL(200)
pBL(60)-IRSL(200)
Normalized signals
Annealing temperature, ˚C
0.0
0.2
0.4
0.6
0.8
1.0
1.2
150
200
250
300
350
400
450
500
550

Figure 9

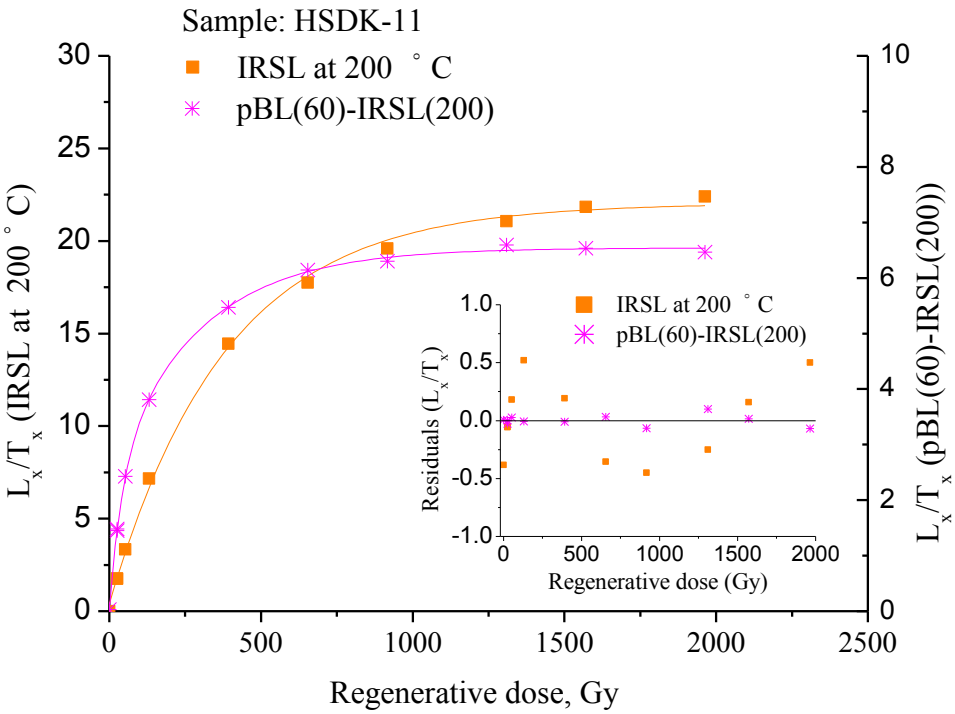
Sample: HSDK-11
IRSL at 200 ° C
pBL(60)-IRSL(200)
L_x/T_x (IRSL at 200 ° C)
L_x/T_x (pBL(60)-IRSL(200))
Regenerative dose, Gy
Residuals (L_x/T_x)
Regenerative dose (Gy)

865

866

867 Figure 10

868

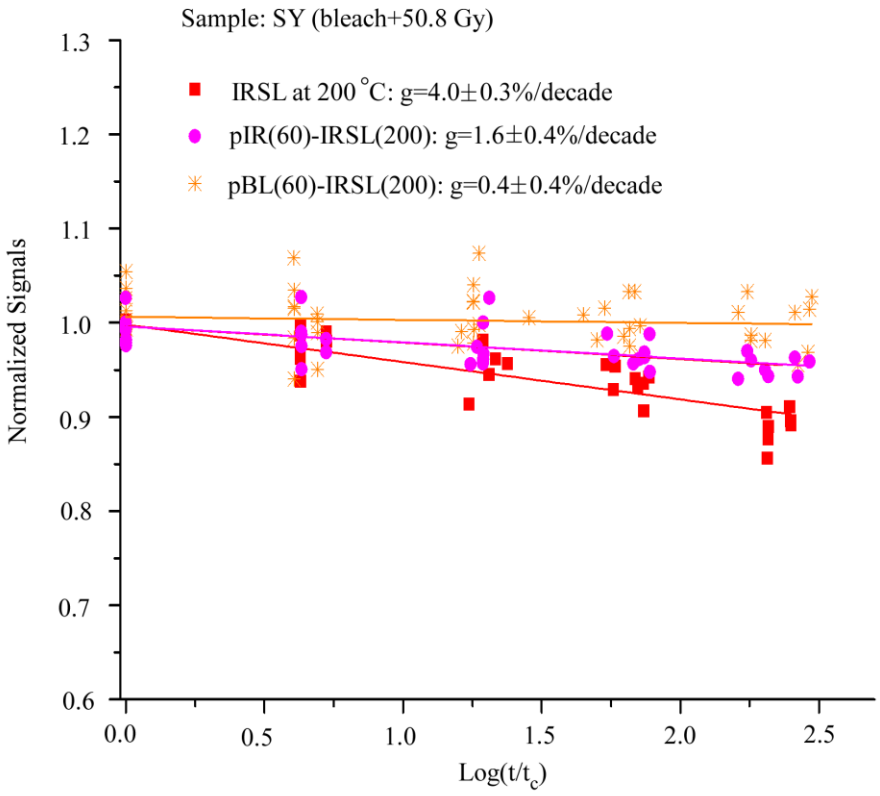

869

870

871

872

873

874

875

876

877

878

879

Table 1

Experimental procedures for the pIR(T_1)-BLSL(T_2) and pBL(T_2)-pIRSL(T_1) experiments. T_1 were set at 60,100, 150, 200 °C respectively, while T_2 were set at 60 and 200 °C.

	pIR(T_1)-BLSL(T_2)		pBL(T_2)-pIRSL(T_1)	
Step	Treatment	Observed	Treatment	Observed
(1)	Cut-heat to 500 °C		Cut-heat to 500 °C	
(2)	Regenerative dose (30.4 Gy)		Regenerative dose (30.4 Gy)	
(3)	Preheat to 280 °C for 10 s		Preheat to 280 °C for 10 s	
(4)	IR bleaching at T_1 for different time (0-5000 s)		BL bleaching at T_2 for different time (0-320 s)	
(5)	BLSL measurement at T_2 for 200 s	$L_{pIR\text{-}BLSL}$	IRSL measurement at T_1 for 160 s	$L_{pBL\text{-}IRSL}$
(6)	Test dose (15.2 Gy)		Test dose (15.2 Gy)	
(7)	Preheat to 280 °C for 10s		Preheat to 280 °C for 10s	
(8)	BLSL measurement at T_2 for 200 s	T_{BLSL}	IRSL measurement at T_1 for 160 s	T_{IRSL}
(9)	Return to step 1 and time for bleaching changes		Return to step 1 and time for bleaching changes	

Table 2

Pulse annealing procedures for the IRSL at 60 °C, the IRSL at 200 °C, the pIR(60)-IRSL(200) and the pBL(60)-IRSL(200). Note that the sequence of IRSL at 60 °C is steps 1, 2, 3, 4, 5a, 6, 7, 8a and 9, the sequence of IRSL at 200 °C is steps 1, 2, 3, 4, 5b, 6, 7, 8b and 9, the sequence of pIR(60)-IRSL(200) is steps 1, 2, 3, 3a, 4, 5b, 6, 7, 8b and 9 and the sequence of pBL(60)-IRSL(200) is steps 1, 2, 3, 3b, 4, 5b, 6, 7, 8b and 9.

Step	Treatment	Observed
(1)	Cut-heat to 500 °C	
(2)	Regenerative dose (30.4 Gy)	
(3)	Preheat to 280 °C for 10 s	
(3a)	IR bleaching at 60 °C for 200 s	
(3b)	BL bleaching at 60 °C for 200 s	
(4)	Cut-heat to T °C (160 °C -500 °C)	
(5a)	IRSL measurement at 60 °C for 160 s	$L_{(IRSL\ 60\ °C)}$
(5b)	IRSL measurement at 200 °C for 160 s	$L_{(IRSL\ 200\ °C)}$
(6)	Test dose (30.4 Gy)	
(7)	Preheat to 280 °C for 10 s	
(8a)	IRSL measurement at 60 °C for 160 s	$T_{(IRSL\ 60\ °C)}$
(8b)	IRSL measurement at 200 °C for 160 s	$T_{(IRSL\ 200\ °C)}$
(9)	Return to step 1 and T = T +20 °C	